Check for updates

Received: 15 February 2026 | Accepted: 15 May 2026

DOI: 10.1002/agj2.70458

Agronomy Journal

ORIGINAL ARTICLE

Climatology and Water Management

Thermal sensitivity and yield of Arabica coffee under climatic variability

Marcus Vinicius Oliveira Noronha[1] | **João Paulo Silva**[2] | **Marcos Augusto Plachi**[3] | **Douglas Martins de Santana**[1] | **Renan Caldas Umburanas**[1] | **José Laércio Favarin**[1] | **Luciana Alvim Santos Romani**[2] | **Silvia Maria Fonseca Silveira Massruhá**[2] | **Durval Dourado Neto**[1]

[1]Crop Science, Esalq/USP, Piracicaba, Brazil

[2]Embrapa Digital Agriculture, Campinas, Brazil

[3]Agronomist, Bela Vista da Fumaça farm, Caconde, Brazil

Correspondence
Marcus Vinicius Oliveira Noronha, Crop Science, Esalq/USP, Piracicaba, SP, Brazil.
Email: marcus.noronha@usp.br

Assigned to Associate Editor David Clay.

Funding information
São Paulo Research Foundation, Grant/Award Number: 2022/09319-9;2023/11113-2

Abstract

Coffee yield is influenced by climatic factors, with temperature and water availability being key determinants. This study aimed to evaluate the effects of climate variability on the yield of Arabica coffee (*Coffea arabica* L.) cultivars across phenological phases and to validate an agrometeorological model at local and regional scales using yield–climate time-series data from the Volcanic Region of Poços de Caldas. The Arabica coffee cultivars Mundo Novo 376/4, Catuaí IAC 144, and Bourbon Vermelho were evaluated across four phenological phases. Pearson's correlation coefficients were applied for each phenological phase and production year between yield and climatic variables, along with the Mann–Kendall test to detect monotonic trends in climatic data. The agrometeorological model was evaluated at different analytical scales and under distinct cultivars and yield scenarios, using historical data from 2011 to 2024. The grain-filling phase was the most sensitive to increasing temperature, while flowering showed a rising warming trend, increasing its vulnerability. Cultivars differed in their thermal and water tolerance, with Bourbon Vermelho showing high vegetative resilience but marked reproductive susceptibility. The model performed well at the regional scale ($R^2 = 0.93$; RMSE = 453 kg ha^{-1}), particularly within the Volcanic Region, but exhibited limited accuracy at the plot scale due to local variability. Estimated yield losses were mainly associated with water deficit, followed by frost events, while thermal penalties were minimal. These results highlight the need

Abbreviations: Ap, atmospheric pressure; AWC, available water capacity; Dpt, dew point temperature; ETp, potential evapotranspiration; ETr, actual evapotranspiration; F1, vegetative growth and foliar bud formation phase; F2, induction and maturation of floral buds phase; F3, flowering and fruit expansion phase; F4, fruit filling phase; GCC, GNU compiler collection; Ky, water-stress sensitivity coefficient; MAE, mean absolute error; pA, estimated yield loss due to cold; pB, estimated yield loss due to high temperature; PBIAS, percent bias; pC, water deficit loss; QT, total estimated loss; RH, relative humidity; RMSE, root mean square error; RUa, average relative humidity; RUm, minimum relative humidity; T, plot scale; Ta, mean air temperature; Tm, minimum air temperature; Tse, thermal sum; Tx, maximum air temperature; VBA, Visual Basic for Applications; Wa, mean wind speed; Wx, maximum wind speed; Ye, estimated yield; Yo, observed yield.

This is an open access article under the terms of the Creative Commons Attribution License, which permits use, distribution and reproduction in any medium, provided the original work is properly cited.
© 2026 The Author(s). *Agronomy Journal* published by Wiley Periodicals LLC on behalf of American Society of Agronomy.

to improve climate-resilience strategies and mitigate the impacts of climate change on coffee cultivation.

Plain Language Summary

Coffee production is strongly influenced by climate, especially temperature and water availability. This study evaluated how climate variability affects the yield of three Arabica coffee cultivars (Mundo Novo 376/4, Catuaí IAC 144, and Bourbon Vermelho) at different stages of development in the Volcanic Region of Poços de Caldas. Data from 2011 to 2024 were analyzed to relate climate and yield and to validate an agrometeorological model. The grain-filling stage showed greater sensitivity to rising temperatures, while flowering showed a warming trend. Water deficit was the main cause of yield losses. The model showed good accuracy at the regional scale but lower performance at the local scale. The results help guide strategies to make coffee production more resilient to climate variability.

1 | INTRODUCTION

Coffee is among the most widely traded agricultural commodities globally. In recent years, global production has increased, reaching approximately 176 million bags in the 2024–2025 crop year, of which about 56.8% corresponds to Arabica coffee (*Coffea arabica* L.), with leading production in countries such as Brazil, Ethiopia, and Colombia (Companhia Nacional de Abastecimento, 2025; ICO, 2026). However, the global market is highly sensitive to external factors, including climatic conditions, economic fluctuations, and geopolitical events, which directly affect prices, supply, and the sector's logistics.

Coffee yield is influenced by factors such as agricultural management, soil fertility and type, cultivar, and, climate (Dias et al., 2024). The latter is the most decisive and challenging factor, since climatic conditions are unpredictable and beyond producers' direct control. This climatic variability, which includes seasonal changes, temperature extremes, humidity fluctuations, and rainfall patterns, has a direct impact on the developmental stages of coffee plant (Dias et al., 2024; Pezzopane et al., 2008).

Detailed meteorological information, combined with phenological data from the plant, has become an essential tool for field planning and decision-making in coffee cultivation (Freitas et al., 2024, 2025). High temperatures, such as above 30°C, during the reproductive phases can cause pollen sterility and increase evapotranspiration, leading to reduced flower set, tissue denaturation, hindered fruit formation, and reduced coffee bean mass. Furthermore, rising temperatures decrease the photosynthetic rate and shorten the duration of phenological periods, affecting crop yield (Streck et al., 2012; Torres et al., 2022).

The way climatic variables act across different phenological stages, from bud formation to fruit filling, and how each cultivar responds to climate, combined with management practices such as pruning, plant density adjustment, pest and disease control, and soil fertility, affects crop yield formation and sustainability (Camargo & Camargo, 2001; Freitas et al., 2024). Understanding how climate uncertainty and projections of global warming in the coming decades will impact coffee yield is strategic for modern coffee production, as they may affect both quality and yield (Dias et al., 2024; Freitas et al., 2024).

Crop modeling applied to predict yields and soil conditions have enabled the development of new strategies for decision-making, price forecasting, policy formulation, and strategic planning for domestic and international markets. In coffee crop, the same principle applies, although research in this area remains relatively limited compared to annual crops and is not always updated to reflect local conditions (Freitas et al., 2025; Valeriano et al., 2018).

The agrometeorological model proposed by Santos and Camargo (2006), which integrates climatic parameters with the crop's phenological stages, constitutes a promising tool for yield prediction, provided that its parameters are adjusted according to the phenological scale and environmental conditions (Camargo & Camargo, 2001; Santos & Camargo, 2006). Several studies have sought to improve the model by introducing new variables, such as CO_2 fertilization, and recalibrating water sensitivity coefficients (Verhage et al., 2017), as well as integrating temporal growth curves for roots, leaf area index, soil water availability, crop coefficients, and new approaches to estimate potential yield based on solar radiation (Freitas et al., 2025). Others have tested the model's reliability using different meteorological data sources, including

14350645, 2026, 3, Downloaded from https://acsess.onlinelibrary.wiley.com/doi/10.1002/agj2.70458 by EMBRAPA - Empresa Brasileira de Pesquisa Agropecuaria, Wiley Online Library on [22/06/2026]. See the Terms and Conditions (https://onlinelibrary.wiley.com/terms-and-conditions) on Wiley Online Library for rules of use; OA articles are governed by the applicable Creative Commons License

surface weather stations and gridded datasets provided by the European Centre for Medium-Range Weather Forecasts and National Aeronautics and Space Administration (Valeriano et al., 2018).

Although machine learning modeling techniques have produced satisfactory results for yield prediction (Aparecido et al., 2022), empirical modeling remains widely used in coffee research. The objective of this study was to assess the effects of climate variability on the yield of Arabica coffee cultivars across phenological phases and to validate an agrometeorological model at local and regional scales using yield–climate time-series data from the Volcanic Region of Poços de Caldas. The study also aimed to validate the model proposed by Santos and Camargo (2006) using two combinations of water sensitivity coefficients under scenarios involving different cultivars, yield levels, and scales of analysis, both local and regional levels.

2 | MATERIALS AND METHODS

2.1 | Study site characterization and data collection

Two distinct yield datasets were used in this study, corresponding to different spatial scales: regional (municipal level) and local (farm plot level—primary data). At the regional scale, aggregated data from the Poços de Caldas Volcanic Region were considered, comprising 12 municipalities: four located in the state of São Paulo (Caconde, Divinolândia, São Sebastião da Grama, and Águas da Prata) and eight in Minas Gerais (Poços de Caldas, Caldas, Botelhos, Cabo Verde, Bandeira do Sul, Ibitiúra de Minas, Andradas, and Campestre). Historical municipal data were obtained from the database of Instituto Brasileiro de Geografia e Estatística (2025), while local data at the plot level were collected at Boa Vista da Fumaça Farm (21°40′37″ S, 46°34′22″ W), located near the border between the states of Minas Gerais and São Paulo, with most of its area within the municipality of Caconde, São Paulo state, Brazil (Figure 1).

The region's climate classification has a Cwb-Köppen mesothermal climate, characterized by a dry winter and a mild, rainy summer, with an average altitude of 1286 m and a hilly to mountainous relief (Alvares et al., 2013; Freitas et al., 2024).

The coffee yield dataset (Y) used in this study was collected over a 14-year time series, from 2011 to 2024. The local data were separated and organized into 26 plots within the property, cultivated with three cultivars: Mundo Novo 376/4, Catuaí IAC 144, and Bourbon Vermelho. At the regional scale, the data encompassed all municipalities included in the Volcanic Region of Poços de Caldas.

To correct for errors caused by variability in plant failure rates within the plots, which ranged from 13% to 1%, the methodology adopted involved working within correlations, expressing yield per plant in kilograms of raw processed coffee beans. This approach allowed for the analysis of the average yield of each plant individually within the correlation study. For model validation, yield was expressed in kilograms per hectare (kg ha^{-1}).

For the collection of climatic variables, public data were obtained from automatic meteorological stations located near the study area (Instituto Nacional de Meteorologia, 2025). The variables included precipitation (R), atmospheric pressure (Ap), dew point temperature (Dpt), maximum air temperature (Tx), mean air temperature (Ta), minimum air temperature (Tm), minimum relative humidity (RUm), average relative humidity (RUa), maximum wind speed (Wx), and mean wind speed (Wa). Climatic data covered a 16-year period (2009–2024) (Figures S1–S3), exceeding the yield dataset by 2 years (2009 and 2010). This additional period was necessary due to the analytical approach adopted, which incorporates climatic variables from the 24 months preceding each harvest, thus including the conditions of the complete phenological cycle corresponding to the first year of the yield dataset (2011).

The thermal sum (Tse), expressed in degree-days, was calculated using the equation proposed by Pezzopane et al. (2008):

$$\mathrm{Tse} = \sum_{i=1}^{n} \left(\mathrm{Ta}_i - \mathrm{Tb}\right) \quad (1)$$

$$\mathrm{Ta}_i = \frac{\mathrm{Tx}_i + \mathrm{Tn}_i}{2} \quad (2)$$

where Tx_i, Tn_i, and Ta_i represent the daily maximum, minimum, and average air temperatures (°C), respectively, and Tb is the lower basal temperature (12°C) (H. P. Carvalho et al., 2011), for each phenological stage.

2.2 | Diagram of the division of phenological stages

The definition and division of each phenological stage studied were based on the framework proposed by Camargo and Camargo (2001). It takes 2 years for Arabica coffee plants to complete their cycle, with each phenological year beginning in early September and ending in late August (Figure 2). The first year is characterized by vegetative phases, during which branch development, induction, and maturation of floral buds occur (phases 1 and 2). In the second year, the plant enters the reproductive period, starting with flowering, followed by fruit expansion, fruit filling, and fruit maturation (phases 3, 4, and 5), and ending with the resting period (phase 6). Despite this distinction, the two phenological years occur simultaneously. In other words, when the coffee plant is in the bean

14350645, 2026, 3, Downloaded from https://acsess.onlinelibrary.wiley.com/doi/10.1002/agj2.70458 by EMBRAPA - Empresa Brasileira de Pesquisa Agropecuaria, Wiley Online Library on [22/06/2026]. See the Terms and Conditions (https://onlinelibrary.wiley.com/terms-and-conditions) on Wiley Online Library for rules of use; OA articles are governed by the applicable Creative Commons License

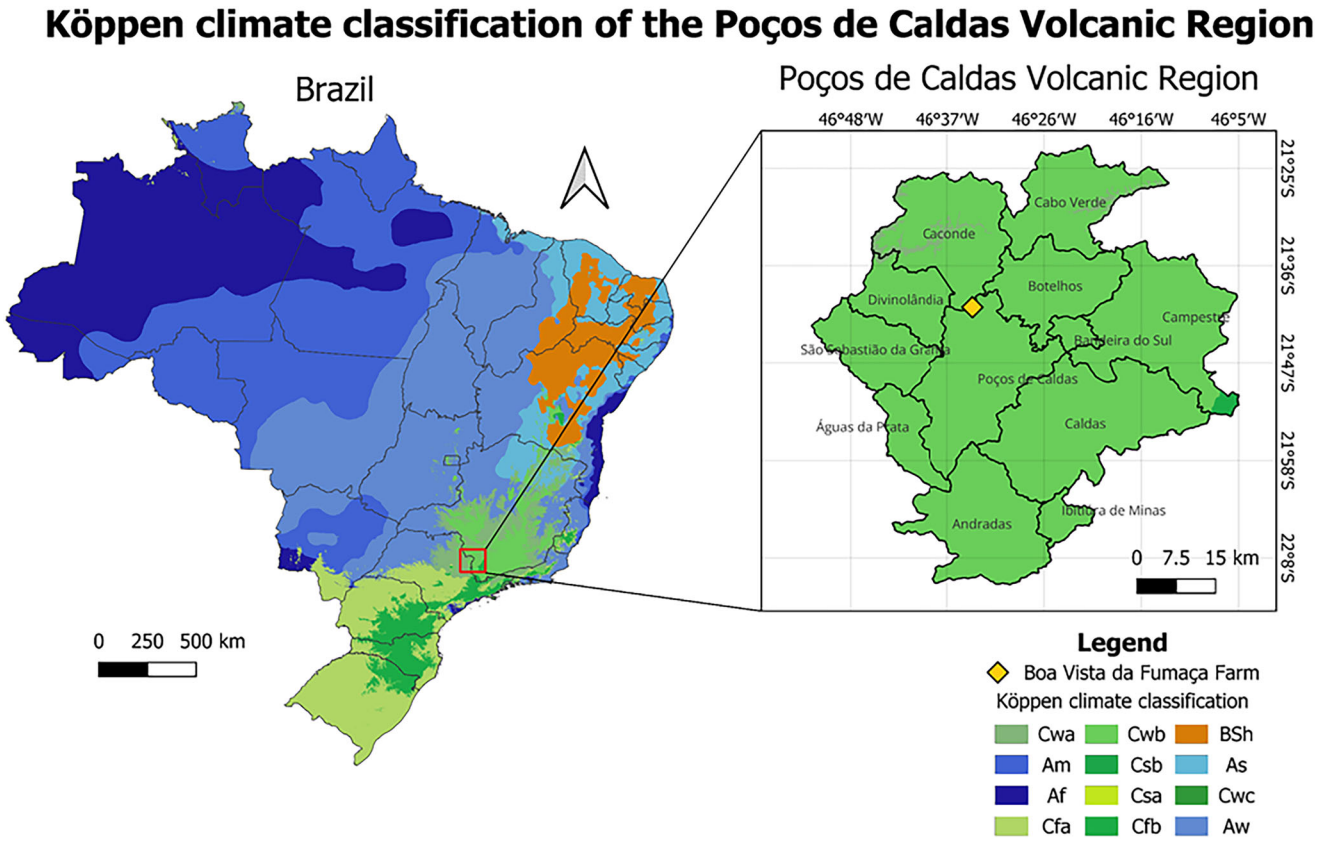


FIGURE 1 Study area: Poços de Caldas Volcanic Region, MG. Adapted from Alvares et al. (2013).

filling stage, it also produces buds that will develop into the following year's crop.

We correlated yield with climatic variables during the periods corresponding to the following key phenological phases: the vegetative growth and foliar bud formation phase (phase 1) (F_1), the induction and maturation of floral buds phase (phase 2) (F_2), the flowering and fruit expansion phase (phase 3) (F_3), and the bean filling phase (phase 4) (F_4), as these are critical stages for determining yield.

2.3 | Correlation between climatic variables and yield

To study and measure the strength of interaction between climatic variables and yield, we used Pearson's correlation coefficients, providing comprehensive insights into the impact of various factors on crop yield (Bhat et al., 2024; Han et al., 2024). The formula is given as follows:

$$P_i = \frac{\sum_{i=1}^{n}\left(X_i - \bar{X}\right)\left(Y_i - \bar{Y}\right)}{\sqrt{\sum_{i=1}^{n}\left(X_i - \bar{X}\right)^2}\sqrt{\sum_{i=1}^{n}\left(Y_i - \bar{Y}\right)^2}} \quad (3)$$

where P_i refers to Pearson's correlation coefficient, X_i represents the climatic variables during the first and second phenological years and the phenological phases (R; Ap; Dpt; Tx; Ta; Tm; RUm; RUa; Wx; Wa; and Tse only in the phenological phases), Y_i represents yield, X^- is the mean of X_i, $\bar{Y}$ is the mean of Y_i, and Σ indicates the summation over all data pairs.

After calculating the Pearson correlations, the results were evaluated using the *t*-test with a significance level of $p < 0.05$ (Bhat et al., 2024), and nonsignificant correlations were removed from the matrix.

2.4 | Climate trend analysis using the Mann–Kendall test

The statistical test developed by Mann (1945) and Kendall (1975) is capable of determining monotonic climate trends, whether increasing, decreasing, or stable, based on the comparison of pairs of observations in a time series.

The test statistic S is calculated by summing the signs of the differences between pairs of observations throughout the series (Equation 4):

$$S = \sum_{j=1}^{n-1}\sum_{k=j+1}^{n} \operatorname{sing}\left(Y_k - Y_j\right), \quad (4)$$

where n represents the total number of observations, Y_k and Y_j represent the data points where $k > j$, j is the index of the

14350645, 2026, 3, Downloaded from https://acsess.onlinelibrary.wiley.com/doi/10.1002/agj2.70458 by EMBRAPA - Empresa Brasileira de Pesquisa Agropecuaria, Wiley Online Library on [22/06/2026]. See the Terms and Conditions (https://onlinelibrary.wiley.com/terms-and-conditions) on Wiley Online Library for rules of use; OA articles are governed by the applicable Creative Commons License

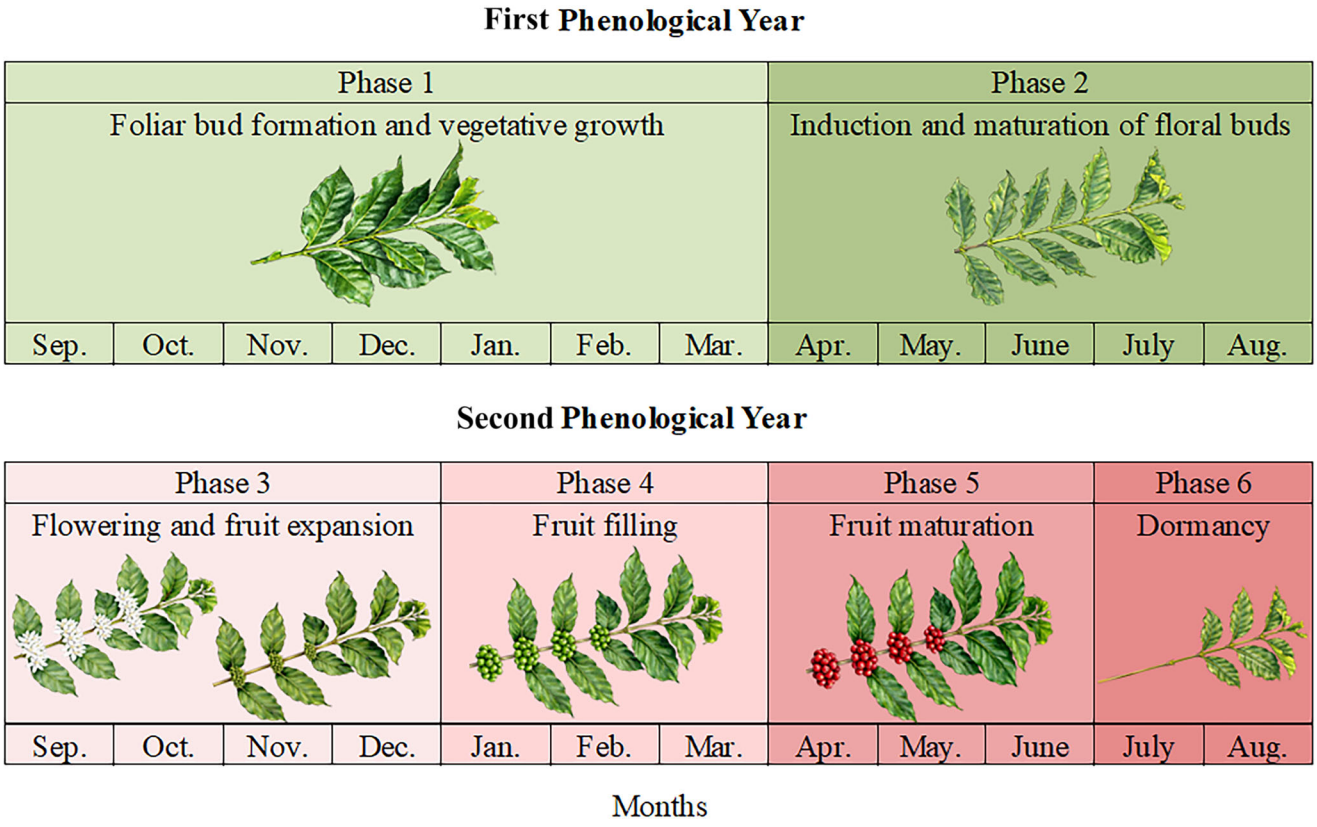


FIGURE 2 Schematic representation of the phenological phases of Arabica coffee over 2 phenological years, as proposed by Camargo and Camargo (2001).

first observation in the pair, and k is the index of the second observation in the pair.

The sign function (Equation 5) determines whether the difference between Y_k and Y_j is positive, negative, or zero. Each pair (Y_k, Y_j) thus contributes +1, 0, or −1 to the total sum S.

$$\text{sing}\left(y_k - y_j\right) = \begin{cases} = +1 \; se \; y_k - y_j > 0 \\ = 0 \; se \; y_k - y_j = 0 \\ = -1 \; se \; y_k - y_j < 0 \end{cases}, \tag{5}$$

The variance of the test statistic S is calculated using the following equation:

$$V \quad (S) = \frac{\{n\,(n-1)\,(2n+5) - \sum_{j=1}^{b}\,[tj\,(tj-1)\,(2tj+5)]\}}{18} \tag{6}$$

where $\sum_{j=1}^{b}$ represents the sum over all groups of tied values, t_j is the number of tied observations in group j, b is the total number of tied groups in the time series, and 18 is the denominator that normalizes the variance of S.

The Z_s statistic determines the statistical significance of the observed trend in the time series, derived from the S statistic and following a standard normal distribution:

$$Z_s = \begin{cases} = \frac{S-1}{\sqrt{V(S)}}, \; S > 0 \\ = 0, \; S = 0 \\ = \frac{S+1}{\sqrt{V(S)}}, \; S < 0 \end{cases}, \tag{7}$$

positive Z_s values indicate increasing trends, negative values indicate decreasing trends, and zero values suggest no trend in the data series. When $|Z_s| > 1.96$, the null hypothesis (H_0) is rejected at a significance level of 0.05, and when $|Z_s| > 2.58$, it is rejected at a significance level of 0.01 (Fattah et al., 2024).

The Kendall coefficient (τ) measures the strength and direction of the monotonic relationship between two variables and is calculated using the following equation:

$$\tau = \frac{S}{\frac{n(n-1)}{2}}, \tag{8}$$

values of τ close to 1 indicate a strong increasing trend, values close to −1 indicate a strong decreasing trend, and values near 0 indicate a weak relationship. The use of this coefficient in the method provides comprehensive insights into the most critical periods concerning yield.

14350645, 2026, 3, Downloaded from https://acsess.onlinelibrary.wiley.com/doi/10.1002/agj2.70458 by EMBRAPA - Empresa Brasileira de Pesquisa Agropecuaria, Wiley Online Library on [22/06/2026]. See the Terms and Conditions (https://onlinelibrary.wiley.com/terms-and-conditions) on Wiley Online Library for rules of use; OA articles are governed by the applicable Creative Commons License

2.5 | Agrometeorological model

The agrometeorological mathematical model developed by Santos and Camargo (2006) consists of phenological, hydric, and thermal parameters, aiming to estimate the relative yield reduction of coffee in the main coffee-growing regions. This model can be represented as follows:

$$Q_{i,j} = \left(1 - \frac{pA_{i,j}}{100}\right) \cdot \left(1 - \frac{pB_{i,j}}{100}\right) \cdot \left(1 - \frac{pC_{i,j}}{100}\right) \cdot 100 \quad (9)$$

where $Q_{(i,j)}$ refers to the total estimated relative loss (%), $pA_{(i,j)}$ refers to the loss estimated due to cold, $pB_{(i,j)}$ refers to the loss estimated due to high temperature, and $pC_{(i,j)}$ refers to the loss estimated due to water deficit, corresponding to the *i*th plot in the *j*th year of the historical series.

The loss estimated due to cold (pA) begins to be accounted for when the absolute minimum temperature (Tma) falls below 2°C at any time of the year (Santos & Camargo, 2006), and the penalty increases sharply as temperature decreases. A temperature near 1°C causes a yield loss of approximately 12%, 0°C causes about 35% loss, −1°C results in 75% loss, and temperatures below −1°C lead to 100% yield loss (Pereira et al., 2008).

The loss due to cold is calculated using the following Gaussian model:

$$pA_{i,j} = 100 \cdot \left(140.3 \cdot e^{\frac{-\left(\mathrm{Tma}_{i,j}+2.96\right)^2}{6.27}}\right), \quad (10)$$

where $pA_{(i,j)}$ refers to the estimated relative yield loss due to cold (%) and $\mathrm{Tma}_{(i,j)}$ $A_{(i,j)}$ refers to the absolute minimum temperature (°C), corresponding to the *i*th plot in the *j*th year of the historical series.

The loss caused by high temperature (pB) is calculated for the first three 10-day periods after full flowering, during which the penalty occurs when the 10-day mean temperature (Tad) exceeds 24°C, which corresponds to a maximum temperature close to 30°C. This penalization factor is calculated using the following equation:

$$pB_{i,j} = 100\left(141.8 \cdot e^{-e^{\left(17.95-0.687\cdot \mathrm{Tad}_{i,j}\right)}}\right), \quad (11)$$

where $pB_{(i,j)}$ refers to the estimated relative yield loss caused by high temperature (%) and $Tad_{(i,j)}$ refers to the 10-day mean temperature (°C), corresponding to the *i*th plot in the *j*th year of the historical series.

The loss caused by water deficit (pC) follows a methodology similar to that of Picini et al. (1999), based on the 10-day water balance calculated according to Thornthwaite and Mather (1955). It considers actual evapotranspiration (ETr), potential evapotranspiration (ETp), and available water capacity (AWC, mm):

$$pC_{i,j} = 100\prod_{d=1}^{n}\left\{\mathrm{Ky_{j,d}}\left(1 - \frac{\mathrm{ETr}_{i,j,d}}{\mathrm{ETp}_{i,j,d}}\right)\right\}, \quad (12)$$

where $pC_{(i,j)}$ refers to the estimated relative yield loss caused by water deficit (%) corresponding to the *i*th plot in the *j*th year; $\mathrm{ETr}_{(i,j,d)}$ and $\mathrm{ETp}_{(i,j,d)}$ refer to actual evapotranspiration (mm) and potential evapotranspiration (mm), respectively, corresponding to the *i*th plot in the *d*th 10-day period of the *j*th year in the historical series; and $Ky_{(j,d)}$ represents the crop water-stress sensitivity coefficient corresponding to the *i*th plot in the *d*th 10-day period.

The model parameterization with the values of the water-stress sensitivity coefficients (Ky) was carried out according to the studies of Santos and Camargo (2006) and Pereira et al. (2008). These values vary for each 10-day period, in accordance with the phenological phases of the coffee plant (Camargo & Camargo, 2001), and impose higher penalties during periods of greater vulnerability to water deficit.

The evolution of the water-stress sensitivity coefficients (Ky) throughout the 10-day periods for two distinct parameterizations presents the following: at the plot scale (T), with higher penalties, and at the regional scale (R), with lower penalties (Figure 3).

In both series, the Ky values remained relatively low from April until full flowering, reflecting the lower sensitivity of the crop to water deficit during the stages of bud maturation and floral induction (Camargo & Camargo, 2001).

From the 10-day period in which full flowering occurs until the second subsequent 10-day period, there is an abrupt increase in the coefficients, characterizing the critical phenological phase for defining coffee crop yield.

During flowering, fruit expansion, and part of grain filling, the coefficients reach their highest values. From mid–grain filling onward, the Ky values gradually decrease until the end of this phase, accompanying the transition to fruit maturation, in which the sensitivity to water deficit is reduced.

The incorporation of the penalization factor for the previous year's yield (fY), proposed by Santos and Camargo (2006), considers (i) the water-stress sensitivity coefficient (Ky) relative to the previous year's yield, (ii) the previous year's yield, and (iii) the empirically calculated record yield:

$$fY_{i,j-1} = \mathrm{Ky}_{i,j-1} \cdot \frac{Y_{i,j-1}}{Y_{10i,j}}, \quad (13)$$

where $fY_{(i,j-1)}$ refers to the penalization factor based on the previous year's yield; $Ky_{(i,j-1)}$ refers to the water-stress sensitivity coefficient relative to the previous year's yield, with values of 1.05 for the plot scale and 0.6 for the regional scale; $Y_{(i,j-1)}$ refers to the previous year's yield (kg ha^{-1}); and $Y_{10(i,j)}$ refers to the yield (kg ha^{-1}) calculated based on the highest yield observed over the last 5 years, increased by 10%, corresponding to the *i*th plot in the *j*th year.

14350645, 2026, 3, Downloaded from https://acsess.onlinelibrary.wiley.com/doi/10.1002/agj2.70458 by EMBRAPA - Empresa Brasileira de Pesquisa Agropecuaria, Wiley Online Library on [22/06/2026]. See the Terms and Conditions (https://onlinelibrary.wiley.com/terms-and-conditions) on Wiley Online Library for rules of use; OA articles are governed by the applicable Creative Commons License

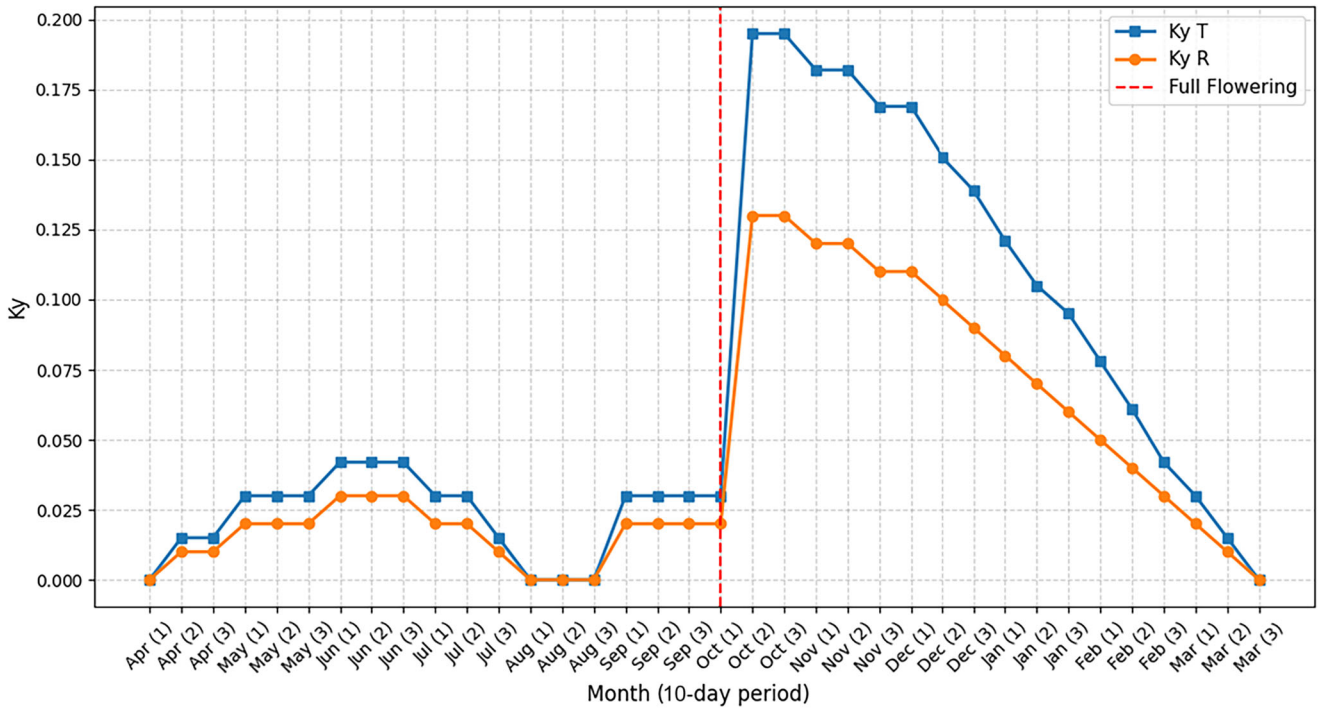


FIGURE 3 Water-stress sensitivity coefficient (Ky), from the first 10-day period of April to the third 10-day period of March, at the plot scale (T) and regional scale (R), before and after full flowering.

The estimated yield was then calculated as follows:

$$Ye_{i,j} = \left(1 - fY_{i,j-1}\right) \cdot Q_{i,j} \cdot Y_{10_{i,j}}, \tag{14}$$

where $Ye_{(i,j)}$ refers to the estimated yield (kg ha^{-1}) corresponding to the *i*th plot in the *j*th year of the historical series.

2.6 | Scenarios and metrics

To evaluate the model's performance, different validation scenarios were defined based on genotypic, productive, and regional characteristics. Through these scenarios, the goal was to test the model's robustness and generalization capacity under different edaphoclimatic conditions.

The scenarios were structured as follows: the complete dataset, encompassing all plots, cultivars, and regions (Scenario A), was designated as the general reference scenario using field-collected data for broad model validation. Specific scenarios were also defined by genotype, Bourbon Vermelho (Scenario B), Catuaí IAC 144 (Scenario C), and Mundo Novo 376/4 (Scenario D), each with distinct agronomic characteristics, allowing the evaluation of the model's sensitivity to different genetic materials.

Additionally, scenarios were established based on the average yield of the plots: yields below 1200 kg ha^{-1} (Scenario E), between 1200 and 1800 kg ha^{-1} (Scenario F), and above 1800 kg ha^{-1} (Scenario G). Generalized regional data from the area of study, known as the Poços de Caldas Volcanic Region (Scenario H), were also used. Each scenario was evaluated at two distinct spatial scales, plot (T) and regional (R), totaling 16 combinations.

2.7 | Computational data analysis

Statistical and computational analyses were performed using the Python programming language (version 3.12.11), compiled with GNU compiler collection (GCC) 11.4.0, employing the *pandas, numpy, scikit-learn*, and *matplotlib* libraries for data processing, regression fitting, and graphical generation. In addition, complementary routines were developed in VBA (Visual Basic for Applications) within Microsoft Excel to automate calculations and organize the spreadsheets used for yield analysis and validation of the agrometeorological model.

3 | RESULTS

3.1 | Climatic variables

Among the various factors that can impact yield, the behavior of the climate in the cultivation systems of the producing regions has proven to be the most damaging and the least controllable, especially temperature, whose increase

14350645, 2026, 3, Downloaded from https://acsess.onlinelibrary.wiley.com/doi/10.1002/agj2.70458 by EMBRAPA - Empresa Brasileira de Pesquisa Agropecuaria, Wiley Online Library on [22/06/2026]. See the Terms and Conditions (https://onlinelibrary.wiley.com/terms-and-conditions) on Wiley Online Library for rules of use; OA articles are governed by the applicable Creative Commons License

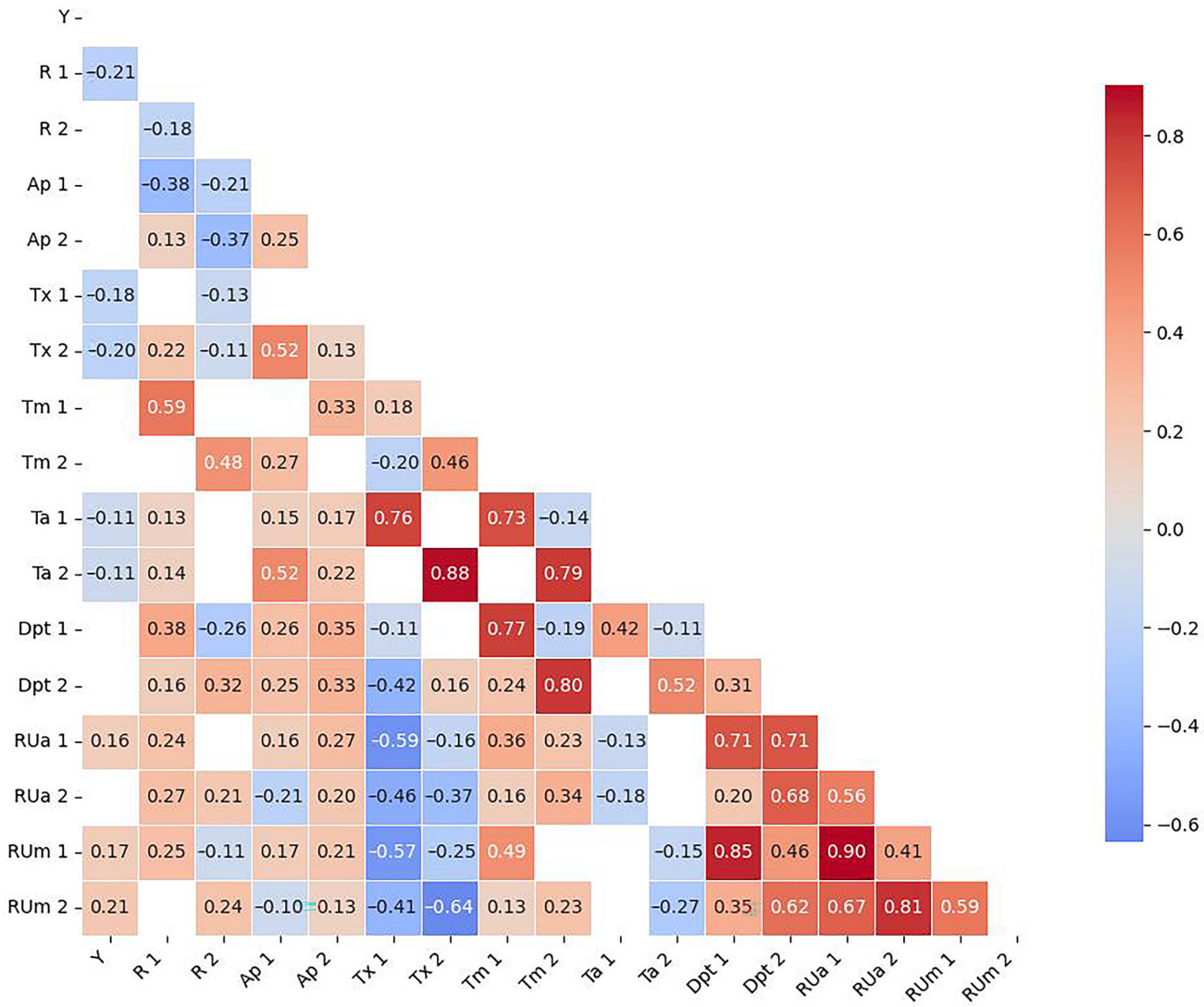


FIGURE 4 Pearson correlation matrix with significant values ($p < 0.05$) between yield (Y) and climatic factors: precipitation (R, mm year^{-1}), atmospheric pressure (Ap, atm), maximum temperature (Tx, ˚C), minimum temperature (Tm, ˚C), average temperature (Ta, ˚C), dew point temperature (Dpt, ˚C), average relative humidity (RUa, %), and minimum relative humidity (RUm, %) in the first (1) and second (2) phenological years of coffee production.

negatively affects several stages of fruit and branch development. Figure 4 details the correlations between climatic variables and coffee yield, highlighting the significant correlations ($p < 0.05$).

There is a weak negative relationship between R1 and yield (−0.21), indicating potential harmful effects of excessive rainfall during the stages of bud formation and development. Temperature was associated with yield in both crop years, covering all phenological stages of coffee. The negative effect was more pronounced in the second year, corresponding to the development of reproductive structures and fruit growth. Negative relationships were observed between yield and both maximum (Tx) (−0.18 and −0.2) and average (Ta) (−0.11 and −0.11) temperatures, especially in the second year, with higher temperature values associated with lower yields.

A positive relationship was also observed between yield and relative humidity (RH). Positive correlations were identified between yield and minimum relative humidity (RUm) in both Years (0.17 and 0.21), as well as with average relative humidity (RUa) in the first year (0.16). In addition, RH showed a moderately negative association with maximum temperature.

In the analysis of yield response for each cultivar as a function of the significant variables (Figure 5), differences were observed in sensitivity to high temperatures and excessive rainfall during the first phenological year, which corresponds to the stages of vegetative growth, bud formation, and maturation of foliar buds (Camargo & Camargo, 2001).

The cultivars Mundo Novo 376/4 and Catuaí IAC 144 were found to be more sensitive, while the Bourbon Vermelho

14350645, 2026, 3, Downloaded from https://acsess.onlinelibrary.wiley.com/doi/10.1002/agj2.70458 by EMBRAPA - Empresa Brasileira de Pesquisa Agropecuaria, Wiley Online Library on [22/06/2026]. See the Terms and Conditions (https://onlinelibrary.wiley.com/terms-and-conditions) on Wiley Online Library for rules of use; OA articles are governed by the applicable Creative Commons License

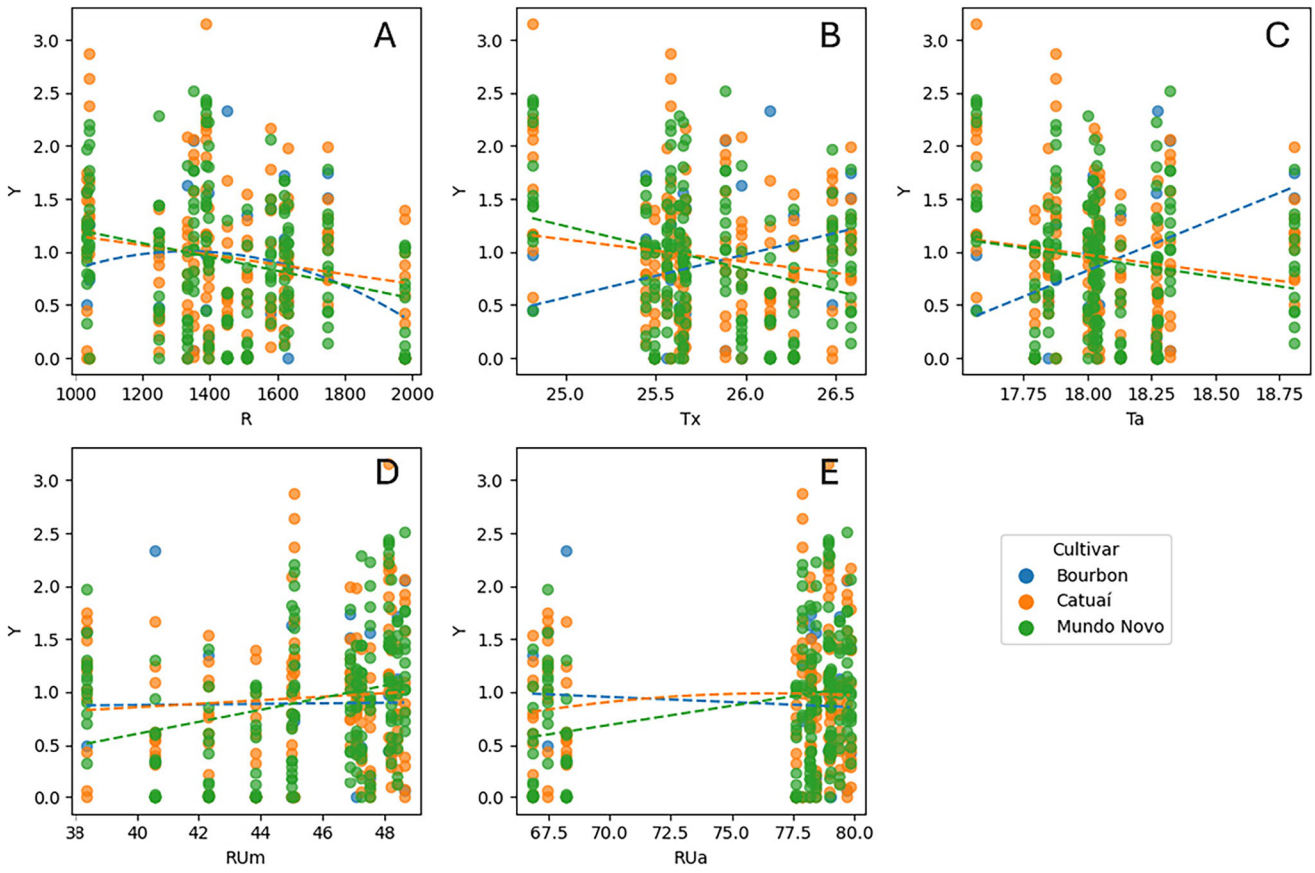


FIGURE 5 Correlation between yield (Y, kg plant^{-1}) and the significant climatic variables: precipitation (R, mm year^{-1}) (A), maximum temperature (Tx, ˚C) (B), average temperature (Ta, ˚C) (C), minimum relative humidity (RUm, %) (D), and average relative humidity (RUa, %) (E) during the first phenological year for the three coffee cultivars (Bourbon Vermelho, Catuaí IAC 144, and Mundo Novo 376/4).

cultivar tolerated higher rainfall volumes and maintained more consistent yield at intermediate levels (Figure 5A), between 1200 and 1800 mm of annual precipitation. Additionally, Bourbon Vermelho showed greater resistance to higher temperatures. The highest yields were observed at an average maximum temperature (Figure 5B) in the first phenological year, between 25.2 and 26˚C. The cultivars Mundo Novo 376/4 and Catuaí IAC 144 appeared to be more negatively affected by rising temperatures, particularly Mundo Novo 376/4, which demonstrated greater sensitivity than the others.

The average temperature (Figure 5C) showed a performance trend like that of Tx, with the highest yields recorded between 17.75 and 18.3˚C. In this regard, the cultivars Mundo Novo 376/4 and Catuaí IAC 144 exhibited very similar responses. They also showed greater variability in yield at higher RH values (Figure 5D,E). For the Bourbon Vermelho cultivar, the slightly negative trend may indicate a potential impact on yield. RH is directly related to Tx (Figure 4), which justifies improvements in the system with higher minimum and average RH, especially for Mundo Novo 376/4 and Catuaí IAC 144.

In the second phenological year, which corresponds to the flowering, development, and fruit filling periods (Camargo & Camargo, 2001), temperature was shown to be the most critical factor affecting yield (Figure 6).

The maximum temperature range (Figure 6A) associated with the highest yields was between 25.4 and 26.5˚C, and the average temperature (Figure 6B) ranged between 17.75 and 18.5˚C. The cultivars Mundo Novo 376/4 and Catuaí IAC 144 exhibited similar behaviors, differing from the Bourbon Vermelho cultivar.

All cultivars showed high sensitivity to elevated temperatures. Bourbon Vermelho demonstrated greater temperature sensitivity during the flowering and fruit development stages compared to the other cultivars and responded better to higher temperatures during the vegetative period. This may indicate that temperature increases are directly related to fruit formation during specific periods of this phase.

The analysis of specific periods such as vegetative growth, bud maturation, flowering, fruit expansion, and fruit filling allows for the identification of phenological stages that are most critical under adverse climatic conditions and that more severely compromise yield. Variables associated with rising temperatures throughout all phenological stages tend to negatively affect yield. Conversely, variables that help mitigate temperature stress tend to be favorable (Figure 7).

14350645, 2026, 3, Downloaded from https://acsess.onlinelibrary.wiley.com/doi/10.1002/agj2.70458 by EMBRAPA - Empresa Brasileira de Pesquisa Agropecuaria, Wiley Online Library on [22/06/2026]. See the Terms and Conditions (https://onlinelibrary.wiley.com/terms-and-conditions) on Wiley Online Library for rules of use; OA articles are governed by the applicable Creative Commons License

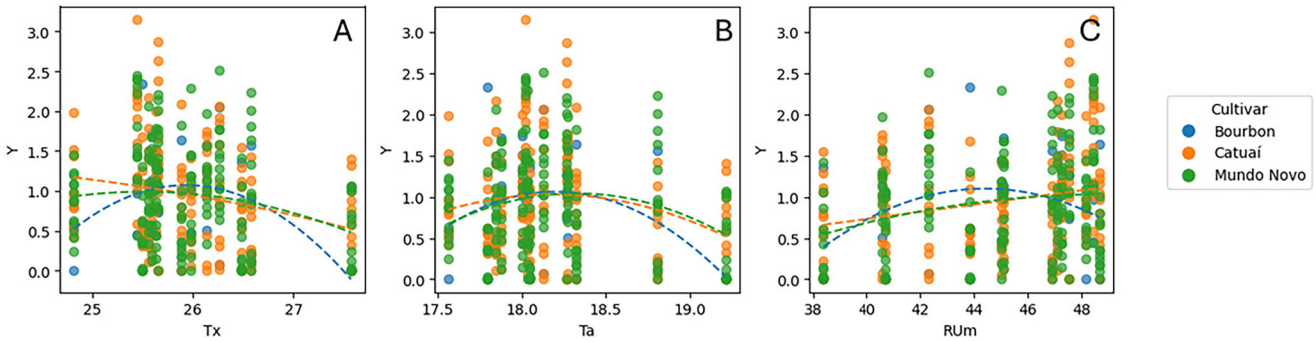


FIGURE 6 Correlation between yield (Y, kg plant^{-1}) and the significant climatic variables: maximum temperature (Tx, ˚C) (A), average temperature (Ta, ˚C) (B), and minimum relative humidity (RUm, %) (C) during the second phenological year for the three coffee cultivars (Bourbon Vermelho, Catuaí IAC 144, and Mundo Novo 376/4).

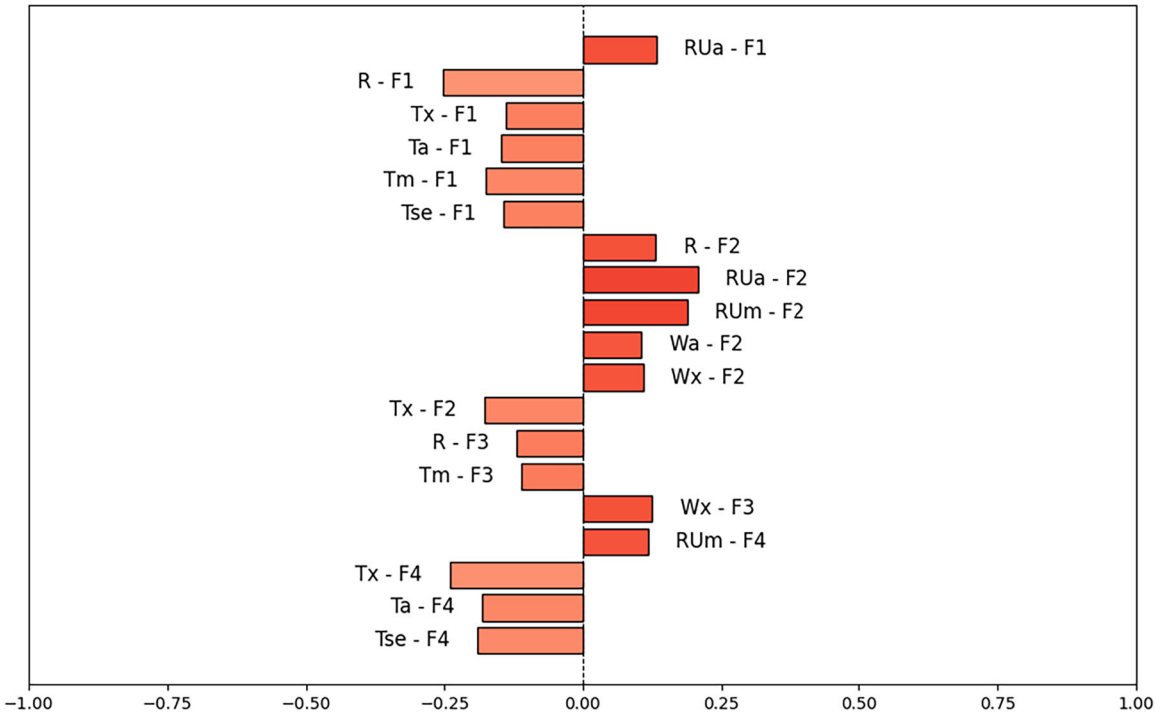


FIGURE 7 Significant correlations ($p < 0.05$) between yield and climatic variables: precipitation (R, mm year^{-1}), maximum temperature (Tx, ˚C), minimum temperature (Tm, ˚C), average temperature (Ta, ˚C), average relative humidity (RUa, %), minimum relative humidity (RUm, %), average wind speed (Wa, m s^{-1}), maximum wind speed (Wx, m s^{-1}), and thermal sum (Ste, ˚C day) during the phases of vegetative growth and foliar bud formation (F1), induction and maturation of floral buds (F2), flowering and fruit expansion (F3), and fruit filling (F4) in coffee plants.

The fruit filling phase (F4) tends to be more sensitive to rising temperatures, as indicated by the more negative correlations of Tx and thermal sum (Tse), suggesting that heat accumulation and high temperatures during this period compromise fruit development. This phase appears to be more critical than the others, even when compared to the flowering and fruit expansion period.

Meanwhile, the effects of minimum temperature (Tm) are more detrimental during the flowering and fruit filling phases. This may be explained by the occurrence of low temperatures extending through the transition from winter to spring and/or in early spring, mainly affecting flowering. Excessive precipitation is also harmful during the flowering period and the maturation of buds; such excess rainfall may stimulate premature flowering (Zacharias et al., 2008) and reduce sunlight incidence during the vegetative period (Roman et al., 2024). The variables that showed positive correlations, except for precipitation during bud maturation (F2), are generally antagonistic to rising temperatures, presenting negative correlations with Tx and Ta. This may be explained by the fact

14350645, 2026, 3, Downloaded from https://acsess.onlinelibrary.wiley.com/doi/10.1002/agj2.70458 by EMBRAPA - Empresa Brasileira de Pesquisa Agropecuaria, Wiley Online Library on [22/06/2026]. See the Terms and Conditions (https://onlinelibrary.wiley.com/terms-and-conditions) on Wiley Online Library for rules of use; OA articles are governed by the applicable Creative Commons License

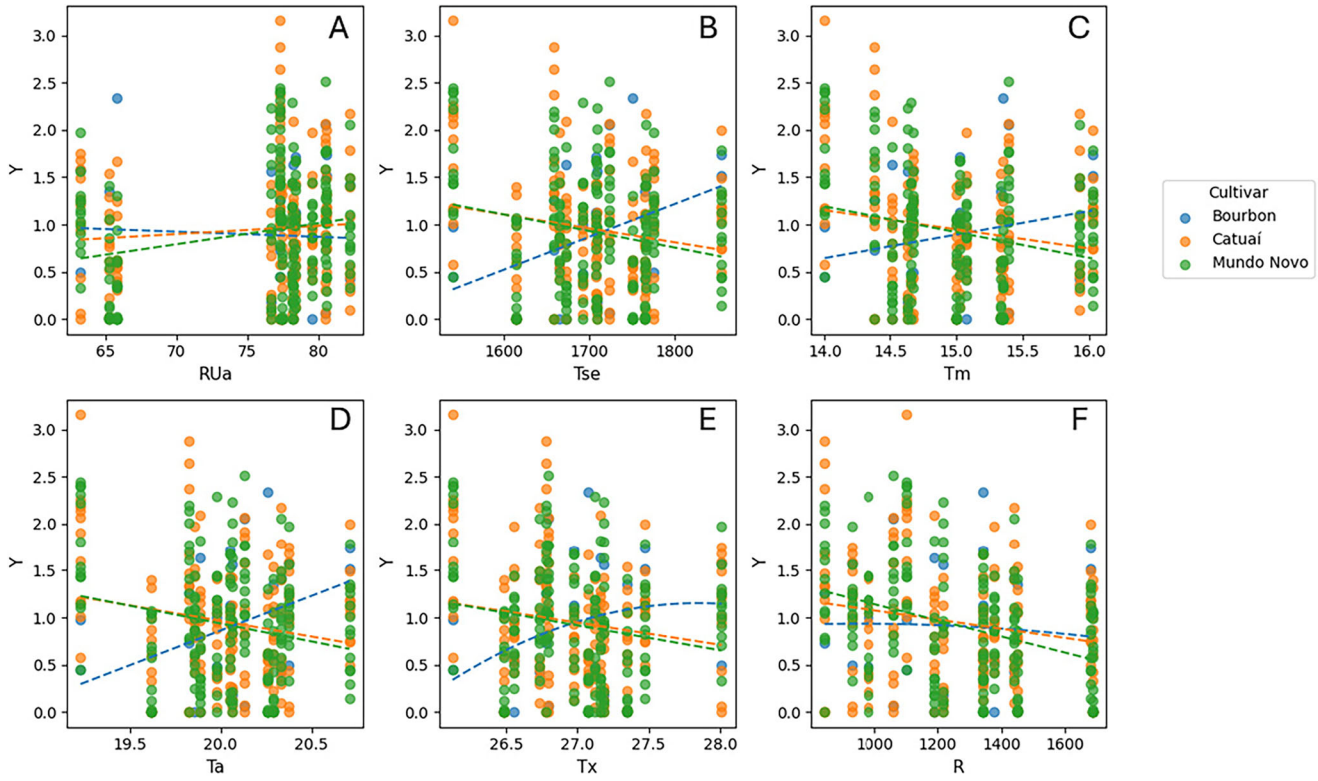


FIGURE 8 Significant correlations ($p < 0.05$) between yield (Y, kg plant^{-1}) and climatic variables: average relative humidity (RUa, %) (A), thermal sum (Tse, ˚C) (B), minimum temperature (Tm, ˚C) (C), average temperature (Ta, ˚C) (D), maximum temperature (Tx, ˚C) (E), and precipitation (R) (F) during the foliar bud formation and vegetative growth phase.

that an increase in these variables contributes to higher yield (Figure 8).

During the bud formation period, the response to higher temperatures was positive for the Bourbon Vermelho cultivar. In contrast, the Catuaí IAC 144 and Mundo Novo 376/4 cultivars showed a decline in yield under thermal stress. The Bourbon Vermelho cultivar was more tolerant to higher values of thermal sum (Figure 8B), minimum temperature (Figure 8C), and average temperature (Figure 8D). However, for maximum temperature (Figure 8E), it maintained stability up to approximately 27.5˚C, whereas the Catuaí IAC 144 and Mundo Novo 376/4 cultivars experienced a reduction in yield as temperature increased. Regarding precipitation (Figure 8F), all cultivars showed decreased yield with high rainfall volumes, but the Mundo Novo 376/4 cultivar was the most adversely affected.

During the bud maturation period (Figure 9), maximum temperatures were milder, and precipitation volumes were lower compared to the previous period. This is due to the seasonality of temperature decline and reduced rainfall, which typically occur during most of the autumn and winter seasons.

Rainier periods, with precipitation above 200 mm during bud maturation, favored yield for the Mundo Novo 376/4 cultivar; however, they negatively affected Bourbon Vermelho (Figure 9C). For Catuaí IAC 144, the increase in rainfall volume had little impact. Higher temperatures during this phase were also detrimental to Mundo Novo 376/4 and Catuaí IAC 144 but beneficial for Bourbon Vermelho, and this is inversely related to the correlations with RUa and Rum. Wind can improve the system; however, excessive wind is harmful to all cultivars. The average wind speed (Figure 9E) shows a constant positive correlation with yield, which is beneficial for increasing yields. Meanwhile, the maximum wind speed (Figure 9D) negatively impacts yield when it exceeds 6.9 m s^{-1}, with an optimal range between 6.7 and 6.9 m s^{-1}.

During the flowering and fruit expansion period (Figure 10), intermediate minimum temperatures (13.5–15˚C) had beneficial effects on all cultivars (Figure 10C). This may be due to the fact that winters and early springs with low temperatures can negatively affect development, particularly flower development. Excessive precipitation during this period also negatively affected the Mundo Novo 376/4 and Catuaí IAC 144 cultivars, while it was beneficial for Bourbon Vermelho (Figure 10A). Meanwhile, minimum temperatures below 13.5˚C and above 14.7˚C caused reductions in yield for all cultivars, as the range between these temperatures resulted in the highest yields (Figure 10B). An increase in Wx was beneficial and showed similar effects across all cultivars.

14350645, 2026, 3, Downloaded from https://acsess.onlinelibrary.wiley.com/doi/10.1002/agj2.70458 by EMBRAPA - Empresa Brasileira de Pesquisa Agropecuaria, Wiley Online Library on [22/06/2026]. See the Terms and Conditions (https://onlinelibrary.wiley.com/terms-and-conditions) on Wiley Online Library for rules of use; OA articles are governed by the applicable Creative Commons License

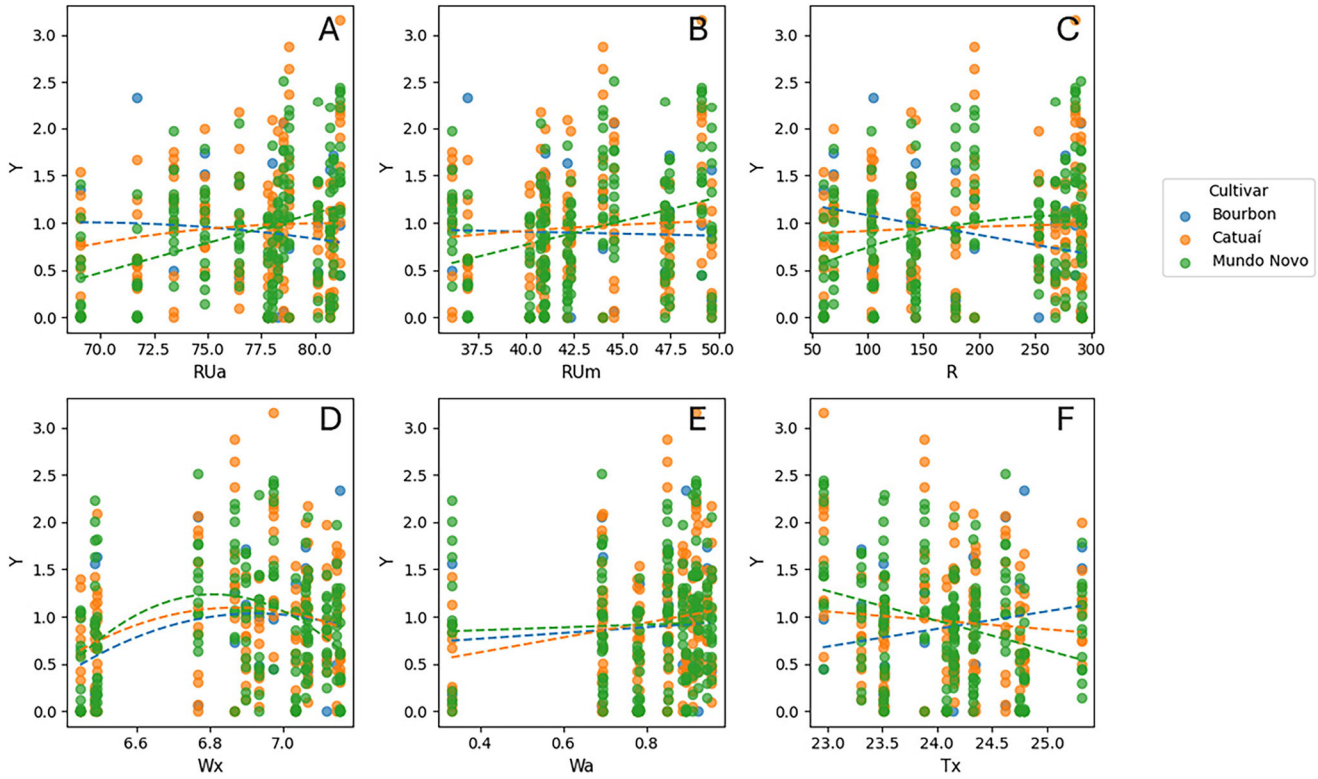


FIGURE 9 Significant correlations ($p < 0.05$) between yield (Y, kg plant^{-1}) and climatic variables: average relative humidity (RUa, %) (A), minimum relative humidity (RUm, %) (B), precipitation (R, mm year^{-1}) (C), maximum wind speed (Wx, m s^{-1}) (D), average wind speed (Wa, m s^{-1}) (E), and maximum temperature (Tx, ˚C) (F) with yield during the bud maturation phase.

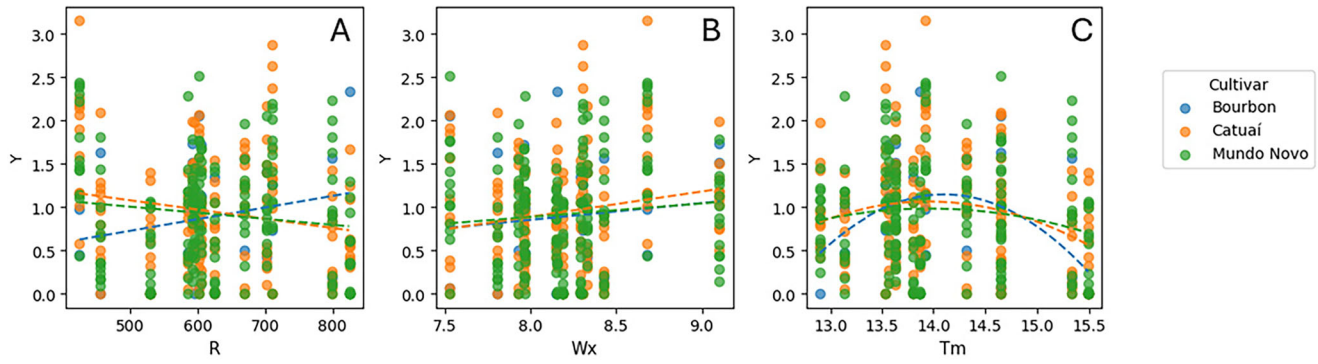


FIGURE 10 Significant correlations ($p < 0.05$) between yield (Y, kg plant^{-1}) and climatic variables: precipitation (R, mm year^{-1}) (A), maximum wind speed (Wx, m s^{-1}) (B), and minimum temperature (Tm, ˚C) (C) during the flowering and fruit expansion phase.

The fruit filling period is the phase that shows the greatest sensitivity to rising temperatures (Figure 11).

Yield shows a negative trend with increasing Ta (Figure 11A) and Tx (Figure 11B) across all cultivars, especially after 20.5˚C for Ta and 27˚C for Tx. The cultivars Mundo Novo 376/4 and Catuaí IAC 144 demonstrated greater stability compared to Bourbon Vermelho, which exhibited higher sensitivity to temperature variation. Minimum RH (Figure 11C) showed a behavior like that observed in the other phenological phases, with a positive correlation with yield. The cultivars Mundo Novo 376/4 and Catuaí IAC 144 achieved higher yield in environments with increased minimum RH. In contrast, Bourbon Vermelho performed poorly under higher RUm conditions.

An increase in thermal sum (Figure 11D) above 750 degree-days had a negative effect on yield, particularly for the Bourbon Vermelho cultivar. The cultivars Catuaí IAC 144 and Mundo Novo 376/4 showed more stable responses and

14350645, 2026, 3, Downloaded from https://acsess.onlinelibrary.wiley.com/doi/10.1002/agj2.70458 by EMBRAPA - Empresa Brasileira de Pesquisa Agropecuaria, Wiley Online Library on [22/06/2026]. See the Terms and Conditions (https://onlinelibrary.wiley.com/terms-and-conditions) on Wiley Online Library for rules of use; OA articles are governed by the applicable Creative Commons License

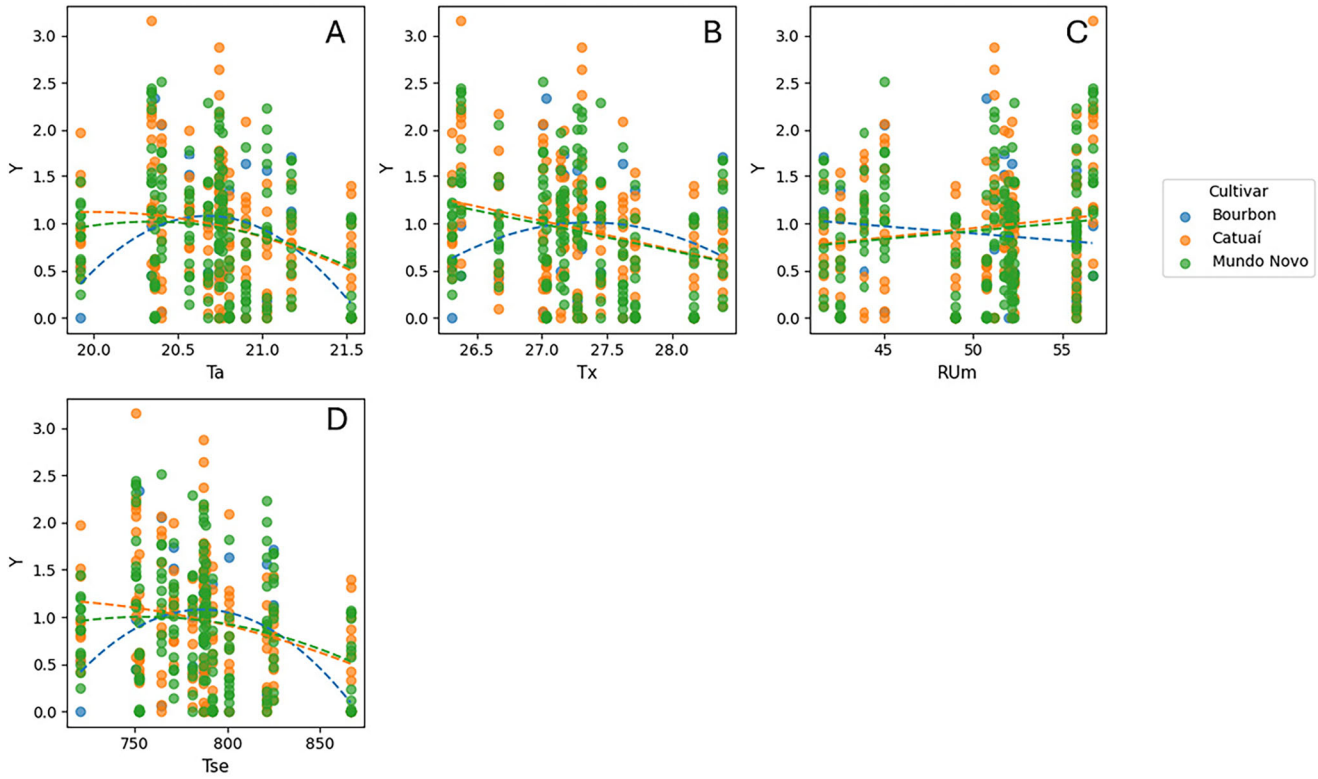


FIGURE 11 Significant correlations ($p < 0.05$) were found between yield (Y, kg plant^{-1}) and climatic variables: mean temperature (Ta, ˚C) (A), maximum temperature (Tx, ˚C) (B), minimum relative humidity (RUm, %) (C), and thermal sum (Tse) (D) during the fruit filling stage.

were more productive within the analyzed range. Overall, the fruit filling period is the most sensitive to rising temperatures compared to the other phenological phases. This is supported by the stronger negative correlations between temperature-related variables and yield (Figure 11).

3.2 | Climatic trends

The results of the Mann–Kendall test detail the trends of climatic variables for each month over the 16-year period (2009–2024) (Figure 12).

Significant positive Z values indicated increasing trends in Tx during March, April, July, and September and in Ta during August, September, and October. The temperature increase is most pronounced in September, as indicated by the higher τ values (0.55 and 0.48) compared to the other months. This temperature increase coincides with the beginning of spring, the period when coffee flowering occurs (September and October) (Camargo & Camargo, 2001), making this phase particularly vulnerable to climate change.

Other months showing increasing trends ($\tau > 0$) in Tx, such as March (0.49), April (0.43), and June (0.52), and in Ta in August (0.46), suggest that autumn and winter seasons tend to become warmer, which may particularly affect the bud maturation period.

The variables RUm, RUa, Dpt, Wx, and Wa showed decreasing trends, especially in December for RUa and RUm ($\tau = 0.65$ and $\tau = 0.72$, respectively), a period when fruits are expanding due to constant cell division (Camargo & Camargo, 2001).

Although the temperature increases in some months where these variables show decreasing trends are not statistically significant, it is possible that temperatures may still rise in these months, since the interaction of these variables is moderately negative with temperature (Figure 12).

In general, climatic trends are mainly related to temperature increases during the bud maturation and flowering and fruit expansion periods, with particular emphasis on the flowering period, which is more susceptible to rising temperature variations.

3.3 | Metrics and efficiency of the agrometeorological model across scenarios

The results obtained from statistical metrics within the analyzed scenarios highlight differences in model performance and reflect variability in its predictive capacity (Figure 13). Despite this variability, all scenarios showed statistical significance based on Pearson's critical values at a 5% significance level.

14350645, 2026, 3, Downloaded from https://acsess.onlinelibrary.wiley.com/doi/10.1002/agj2.70458 by EMBRAPA - Empresa Brasileira de Pesquisa Agropecuaria, Wiley Online Library on [22/06/2026]. See the Terms and Conditions (https://onlinelibrary.wiley.com/terms-and-conditions) on Wiley Online Library for rules of use; OA articles are governed by the applicable Creative Commons License



FIGURE 12 Climatic trends of average relative humidity (RUa, %), minimum relative humidity (RUm, %), maximum temperature (Tx, ˚C), minimum temperature (Tm, ˚C), average temperature (Ta, ˚C), dew point temperature (Dpt, ˚C), precipitation (R, mm year^{-1}), atmospheric pressure (Ap, atm), maximum wind speed (Wx, m s^{-1}), and average wind speed (Wa, m s^{-1}) over a 16-year period, based on the Mann–Kendall statistical test. The numbers from 1 to 12 represent the months (January to December). Green rectangles indicate significant decreasing trends, blue rectangles indicate significant increasing trends, and gray rectangles indicate nonsignificant trends. Z represents the test statistic, and τ is Kendall's coefficient, which measures the strength of the association between time and the climatic variable.

The mean absolute error (MAE) and root mean square error (RMSE) values varied considerably among the scenarios. Some scenarios showed higher values, indicating greater mean absolute deviation from the observed data, particularly at the plot scale (T), reaching up to 1717.5 kg ha^{-1} for MAE and 1943 kg ha^{-1} for RMSE (BT scenario). Conversely, in the regional-scale (R) scenarios, the error values were consistently lower, with the HR scenario standing out for having the lowest MAE (380 kg ha^{-1}) and RMSE (453 kg ha^{-1}) values in the analyzed set.

The R^2 performances also varied, with some scenarios showing values above 0.9 (HT and HR), indicating a strong explanatory capacity of the model in relation to the data. However, most scenarios presented values below 0.6, revealing the model's limited ability to explain the results in those cases. Meanwhile, the ET and GR scenarios showed intermediate results, with R^2 values of 0.67 and 0.66, respectively. The R^2 values and the correlations between observed yield (Yo) and estimated yield (Ye) followed similar patterns, with some scenarios showing correlations above 0.9 (HT and HR),

14350645, 2026, 3, Downloaded from https://acsess.onlinelibrary.wiley.com/doi/10.1002/agj2.70458 by EMBRAPA - Empresa Brasileira de Pesquisa Agropecuaria, Wiley Online Library on [22/06/2026]. See the Terms and Conditions (https://onlinelibrary.wiley.com/terms-and-conditions) on Wiley Online Library for rules of use; OA articles are governed by the applicable Creative Commons License

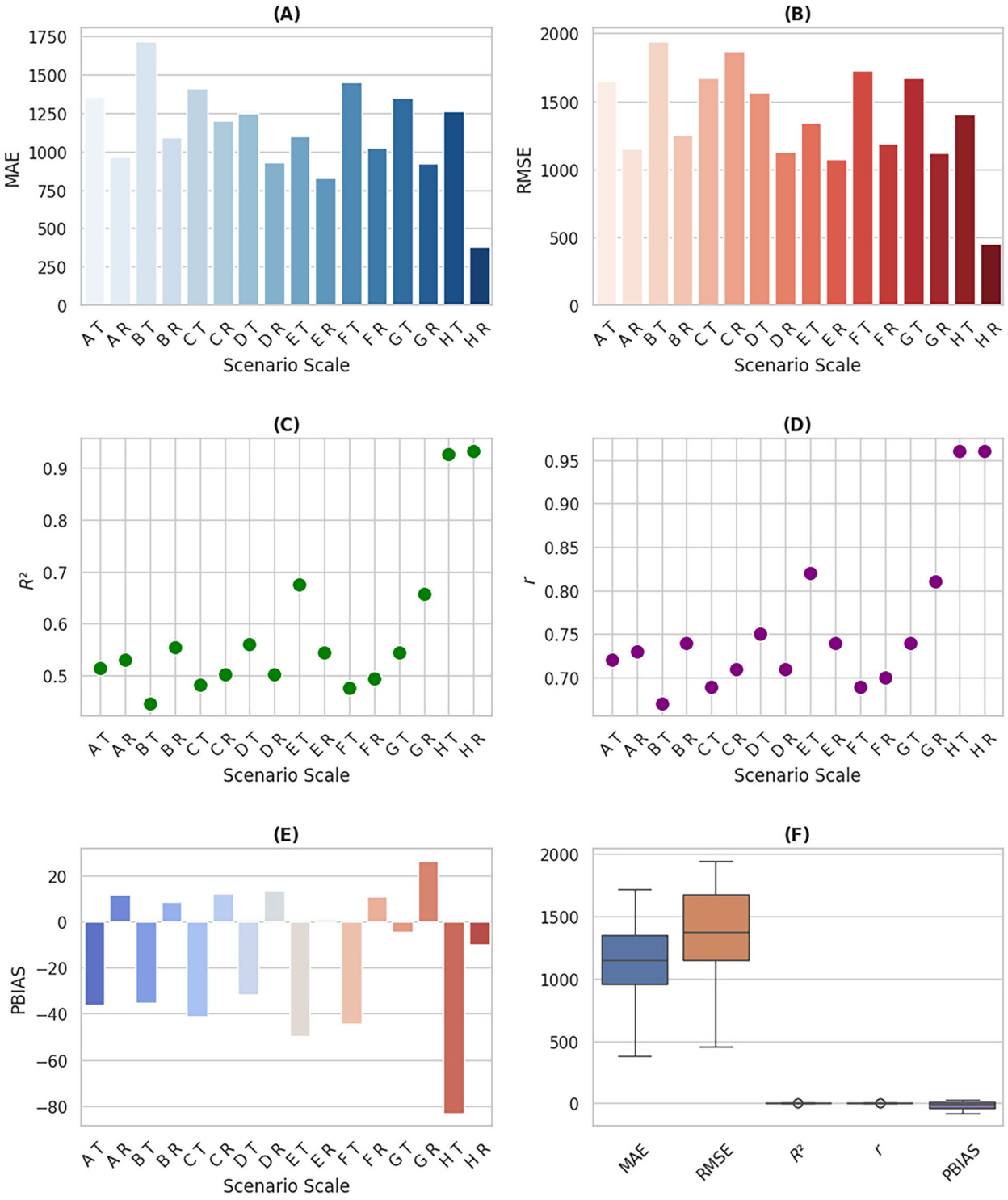


FIGURE 13 (A) Mean absolute error (MAE, kg ha^{-1}), (B) root mean square error (RMSE, kg ha^{-1}), (C) coefficient of determination (R^2), (D) correlation coefficient (r), (E) percent bias (PBIAS, %), and (F) distribution of the overall set of statistical metrics across the following scenarios at the plot (T) and regional (R) scales: (Scenario A) cultivars Catuaí IAC 144, Mundo Novo 376/4, and Bourbon Vermelho considering all plots; (Scenario B) cultivar Bourbon Vermelho considering all plots; (Scenario C) cultivar Catuaí IAC 144 considering all plots; (Scenario D) cultivar Mundo Novo 376/4 considering all plots; (Scenario E) cultivars Catuaí IAC 144, Mundo Novo 376/4, and Bourbon Vermelho considering plots with average yield below 1200 kg ha^{-1}; (Scenario F) cultivars Catuaí IAC 144, Mundo Novo 376/4, and Bourbon Vermelho considering plots with average yield between 1200 and 1800 kg ha^{-1}; (Scenario G) cultivars Catuaí IAC 144, Mundo Novo 376/4, and Bourbon Vermelho considering plots with average yield above 1800 kg ha^{-1}; and (Scenario H) cultivars Catuaí IAC 144, Mundo Novo 376/4, and Bourbon Vermelho considering plots within the Poços de Caldas Volcanic Region.

14350645, 2026, 3, Downloaded from https://acsess.onlinelibrary.wiley.com/doi/10.1002/agj2.70458 by EMBRAPA - Empresa Brasileira de Pesquisa Agropecuaria, Wiley Online Library on [22/06/2026]. See the Terms and Conditions (https://onlinelibrary.wiley.com/terms-and-conditions) on Wiley Online Library for rules of use; OA articles are governed by the applicable Creative Commons License

indicating a strong linear relationship between observed and estimated values. Other scenarios, such as BT, CT, FT, and FR, showed weaker correlations, below 0.7, which reflected lower predictive performance.

The percent bias (PBIAS) values also showed high variability, indicating both underestimation (>0) and overestimation (<0) of actual values. Scenarios evaluated at the plot scale tended to overestimate, while those at the regional scale tended to underestimate, except for HR, which exhibited a negative PBIAS (%). Some scenarios presented satisfactory values (<±25%) (J. Wu et al., 2019), such as BR, ER, GT, and HR (<±10%) and AR, CR, DR, and FR (between ±10% and ±25%), indicating better model performance.

Meanwhile, several scenarios showed unsatisfactory values (>±25%), such as AT, BT, DT, and GR (between ±25% and ±40%), as well as CT, ET, FT, and HT (>±40%), ranging from 26% (GR) to −83% (HT), suggesting low model accuracy in these cases. The scenarios at the plot scale showed poorer PBIAS performance, similar to the MAE and RMSE results, indicating that this scale has lower predictive efficiency.

In general, the analyzed scenarios showed notable variations across all metrics, with high error values in most cases, except for the HR scenario, where the model demonstrated good performance in terms of R^2, r, errors, and bias.

3.4 | Losses estimated by the model in the dataset

Total estimated loss (QT) was systematically higher at the plot scale compared to the regional scale (QR), which can be attributed to the greater penalization imposed by the model (Figure 14). Among the variability in losses, the 2016 growing season showed the greatest variation, with substantially reduced total losses at both scales. Conversely, the years 2017 and 2021 exhibited the highest attributed losses, with modest variations mainly caused by water deficit loss (pC) compared to the other years.

pC were higher and more variable, reaching peaks in 2017 and 2021, with more than 20% losses at the plot scale. At the regional scale, values ranged between 5% and 15%, showing a similar pattern to the plot scale but with lower magnitude, with losses around 15% in those respective years. Meanwhile, estimated yield loss due to high temperatures (pB) remained stable throughout the time series, with nearly null values except in 2024, when a slight variation was observed at both levels. Estimated yield loss due to cold (pA) were the most significant, showing consistently high values except in 2016, which presented a decrease compared to other years, likely attributable to higher and less severe minimum temperatures.

In general, the total losses closely followed the variations in pC and, to a lesser extent, the variations in pA. This indicates that the model identifies pC as the main determinant of the variability in climate-induced yield losses.

4 | DISCUSSION

4.1 | Climatic sensitivity of the cultivars used

The negative relationship observed between temperature and yield, particularly in the second phenological year, may be associated with increased water demand during critical stages such as fruit development and filling, which are characterized by higher potential evapotranspiration intensified by rising temperatures (Humphries et al., 2024; Thornthwaite, 1948).

Phenological stages with higher water demand are more sensitive to this increase, which explains the lower (more negative) coefficients of temperature-related variables during the fruit filling period. The temperature rise during this period also affects foliar bud development, as it largely coincides with this phase (Camargo & Camargo, 2001).

The difference in cultivar sensitivity to temperature increases is evident, particularly for the Bourbon Vermelho cultivar during phases 1 and 2, where higher temperatures favor vegetative development, making it more resistant in this period. This resistance may occur because this cultivar has thick cuticles and palisade parenchyma, as well as smaller stomata, which reduce evapotranspiration and favor greater carbohydrate production during vegetative periods (Batista et al., 2010).

Meanwhile, Bourbon Vermelho is the cultivar that shows the greatest sensitivity to temperature variation during the flowering, cell division, and fruit filling periods, and coincidentally, has the lowest average yield. This sensitivity may be related to increased water demand during this period, which is more critical during grain filling (Du et al., 2020). Combined with the high stomatal density present in its leaves compared to other cultivars (Batista et al., 2010), Bourbon Vermelho becomes inefficient in water use during periods of greater water demand.

Rainfall volumes during phases 1, 2, and 3 also affected the production of some cultivars, with higher volumes, especially during the bud formation period, being more detrimental to all cultivars. Increased precipitation is directly related to soil oxygenation, and excess rainfall can result in oxygen deficiency, leading to reduced root activity and net photosynthetic rate, which ultimately results in lower biomass accumulation during vegetative periods (Liu et al., 2015; F. Wu et al., 2024).

Temporary lack of soil oxygenation leads to nutrient unavailability, commonly causing iron and manganese deficiencies following high rainfall events. Although this deficiency can lower the soil's redox potential, promoting the reduction of Fe^{3+} to Fe^{2+} and Mn^{4+} to Mn^{2+}, thereby increasing nutrient availability, plants exhibit induced

14350645, 2026, 3, Downloaded from https://acsess.onlinelibrary.wiley.com/doi/10.1002/agj2.70458 by EMBRAPA - Empresa Brasileira de Pesquisa Agropecuaria, Wiley Online Library on [22/06/2026]. See the Terms and Conditions (https://onlinelibrary.wiley.com/terms-and-conditions) on Wiley Online Library for rules of use; OA articles are governed by the applicable Creative Commons License

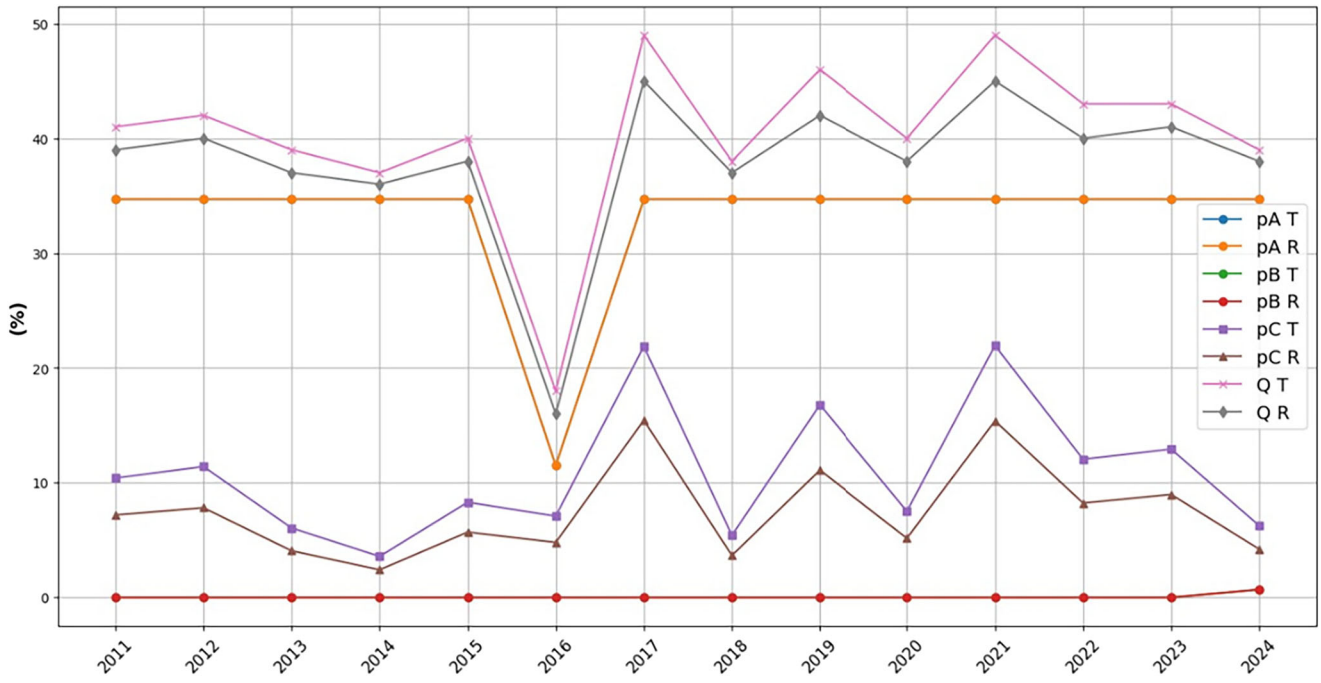


FIGURE 14 Estimated losses (%) due to cold (pAT and pAR), high temperatures (pBT and pBR), water deficit (pCT and pCR), and total estimated loss (QT and QR) at the plot (T) and regional (R) scales.

inefficiency in nutrient absorption due to nutritional imbalances, metabolic inhibition, and/or tissue damage. This is further exacerbated in acidic soils, like those in the study areas, where the oxidation-reduction processes are not as decisive for nutrient availability, intensifying the deficiency (Mehrotra et al., 2022; Shuman, 2005).

Excessive moisture from high precipitation also promotes the incidence and severity of diseases (Salazar-Navarro et al., 2024), which justifies the sensitivity during the flowering period for the Catuaí IAC 144 and Mundo Novo 376/4 cultivars, especially to common diseases during this period, such as Phoma (*Phoma* spp.) and bacterial blight (*Pseudomonas garcae*) (Dias et al., 2024; Monteiro, 2009).

Excessive rainfall also increases the number of cloudy days, which are directly related to reduced sunlight, potentially impacting carbohydrate production (Xie & Li, 2020).

The correlations between yield and RH values (RUa and RUm) are inversely proportional to correlations with temperature (Tx and Ta), indicating that temperature increases are directly related to reductions in RH. Similar results were obtained by Dias et al. (2024), who analyzed the risks of climate change in Arabica coffee-growing regions under future climate projections, where increased temperatures are reflected in lower RH. This reduction may potentially benefit Catuaí IAC 144 and Mundo Novo 376/4 cultivars during the vegetative period and all cultivars during the reproductive period.

The effect of wind is associated with heat exchange with the environment, promoting temperature reduction and increasing crop evapotranspiration (Monteiro, 2009).

Wind can be beneficial during bud maturation and the flowering and fruit expansion phases, possibly due to improved thermal sensitivity, especially during flowering. However, stronger winds tend to be detrimental during bud maturation, being associated with milder winter temperatures and potentially promoting the spread of diseases, particularly Phoma leaf spot (*Phoma* spp.) (Monteiro, 2009).

4.2 | Climatic variations

Future climatic variations in Brazilian coffee-growing regions, as studied by Dias et al. (2024), using climate prediction modeling system models for different periods throughout the 21st century, indicate significant temperature increases and reductions in RH in most of the regions analyzed. These findings are consistent with the results obtained in this study, which applied Mann–Kendall trend analysis. The temperature increase, particularly during the flowering phase, may alter coffee production strategies in the region in the coming years, exposing this phase to greater climatic vulnerability.

Excessive temperature during flowering can cause a series of negative impacts on the development of reproductive organs. One of the main effects is the abortion of flower buds, which reduces the number of viable flowers and, consequently, fruit set. Additionally, high temperatures can either advance flowering or delay it under conditions of severe water deficit, resulting in early and uneven flowering events (Freitas et al., 2024; Pereira et al., 2008; Tavares et al., 2018).

14350645, 2026, 3, Downloaded from https://acsess.onlinelibrary.wiley.com/doi/10.1002/agj2.70458 by EMBRAPA - Empresa Brasileira de Pesquisa Agropecuaria, Wiley Online Library on [22/06/2026]. See the Terms and Conditions (https://onlinelibrary.wiley.com/terms-and-conditions) on Wiley Online Library for rules of use; OA articles are governed by the applicable Creative Commons License

This phenomenon disrupts the synchronicity of the production cycle, causing fruits to mature at different times, which complicates harvesting and reduces coffee uniformity. Consequently, there is a direct impact on crop yield and the quality of the next harvest. Beyond physiological alterations, increased temperatures can intensify pest and disease pressures, such as coffee leaf miner (*Leucoptera coffeella*, Guérin-Mèneville) and coffee leaf rust (*Hemileia vastatrix*, Berkeley and Broome). Meanwhile, it may reduce the incidence of Phoma, brown eye spot (*Cercospora coffeicola*, Berkeley and Cooke), and coffee berry borer (*Hypothenemus hampei*, Ferrari) (Dias et al., 2024).

Climatic trends indicate rising temperatures during winter and early spring, which aligns with historical data and future projections for coffee regions with a Cwa climate, corroborating results observed by Freitas et al. (2024), who also indicated temperature increases for most coffee-growing areas under future scenarios.

This warming directly impacts coffee phenology, accelerates fruit maturation, and disrupts the plant's reproductive cycle, particularly flowering. Early maturation may compromise bean quality by reducing the time required for full fruit development. Late flowering can result in irregular fruit distribution, leading to uneven harvests and creating challenges in crop management and harvesting operations. Meanwhile, this warming may reduce the incidence of frost, potentially making cultivation viable in lower and flatter regions (Dias et al., 2024; Freitas et al., 2024). Adaptive measures, such as using more heat-tolerant varieties and adjusting water and nutrient management practices, may be key strategies for producers in the region to ensure greater production resilience in the face of environmental changes.

4.3 | Agrometeorological model

The analysis of the evaluated scenarios revealed significant variations in the model's performance across different scales and cultivation conditions. The metrics used (MAE, RMSE, R^2, correlation coefficient r, and PBIAS) allowed not only the assessment of the model's overall effectiveness but also the identification of its limitations under specific contexts (Freitas et al., 2025; Santos & Camargo, 2006; Verhage et al., 2017). In terms of evaluation scales, the model demonstrated superior performance in the regional-scale scenarios compared to those at the plot scale.

This is because the combined Ky values are lower at the regional scale, which also explains the better performance observed in the scenario involving the Volcanic Region, due to the greater homogenization of coffee yield across different cultivation systems, representing average production per area, and the reduced influence of biennial bearing (Pereira et al., 2008). These results suggest that the model exhibits greater predictive capacity when applied to larger spatial aggregations, as a consequence of the smoothing of local variations and specific noise.

In the remaining scenarios, particularly at the plot scale, low predictive accuracy was observed. The unsatisfactory performance in scenarios such as BT, CT, and FT, with R^2 values below 0.5 and high MAE and RMSE values, demonstrates the model's difficulty in capturing nuances in yield, which is consistent with the findings reported by L. G. Carvalho et al. (2003). This limitation becomes more evident in the PBIAS analysis, where the largest deviations (such as −83% in scenario HT) reinforce the model's tendency to overestimate or underestimate predicted values (J. Wu et al., 2019).

In the cultivar-based evaluation (Scenarios B, C, and D), the model also showed similar behavior across scales, although without achieving satisfactory performance in any of the cases. Such behavior may indicate that, under the studied Ky combinations, the model does not efficiently account for the productive particularities of different cultivars. In the scenarios grouped by average yield (Scenarios E, F, and G), the model presented more consistent performance, and to some extent, the application to more homogeneous yield ranges favored model performance, except in the intermediate range.

The analysis of the overall distribution of the metrics also revealed a strong statistical discrepancy among the scenarios, reinforcing the variability in the model's efficiency. This heterogeneous performance highlights the importance of stratifying by region, cultivar, or yield class when calibrating and validating predictive models. Several studies have demonstrated the effectiveness of the proposed model (Freitas et al., 2025; Valeriano et al., 2018; Verhage et al., 2017), emphasizing the use of standardized yield data at municipal and regional scales. In these studies, the authors proposed improvements to the model (Freitas et al., 2025; Verhage et al., 2017), as well as the use of different meteorological data sources (Valeriano et al., 2018).

Regarding the estimated losses, the model identified frost-related losses as the most significant. The frost penalization factor is calculated as a function of the absolute minimum temperature (below 2°C); temperatures above 2°C do not cause yield losses, but when temperatures drop below this threshold, losses increase sharply, reaching 12% at 1°C, 35% at 0°C, 75% at −1°C, and total loss at even lower temperatures (Pereira et al., 2008; Santos & Camargo, 2006). In the studied area, frost-related losses remained constant over the years, except in 2016, which recorded minimum temperatures near 2°C. The high yield losses caused by frost are attributed to the crop's vulnerability to low temperatures, which induce severe and irreversible damage to plant tissues due to freezing (Bussoni et al., 2022; Dias et al., 2024). Conversely, excessive temperatures did not cause significant losses, except in 2024, when a slight loss of 0.8% was observed, indicating 10-day

14350645, 2026, 3, Downloaded from https://acsess.onlinelibrary.wiley.com/doi/10.1002/agj2.70458 by EMBRAPA - Empresa Brasileira de Pesquisa Agropecuaria, Wiley Online Library on [22/06/2026]. See the Terms and Conditions (https://onlinelibrary.wiley.com/terms-and-conditions) on Wiley Online Library for rules of use; OA articles are governed by the applicable Creative Commons License

periods with the mean temperatures above 24°C (Pereira et al., 2008).

Water deficit was the main fluctuating factor in yield losses across the years and scales studied, with relatively higher losses observed in 2007 and 2021. Unlike temperature-related losses, penalizations due to water deficit can vary according to the combinations of sensitivity coefficient series used for parameterization and the estimated period of full flowering of the crop (Freitas et al., 2025; Pereira et al., 2008; Santos & Camargo, 2006), which explains the differences in losses between the plot and regional levels. In addition, periods with reduced rainfall and higher temperatures increase the gap between potential and actual evapotranspiration (Thornthwaite, 1948), thereby intensifying pC.

The results confirm that the model's effectiveness, given the Ky coefficients used, is directly related to the scale of application and the homogeneity of the data. The better performance at the regional scale demonstrates the potential of the modeling approach for strategic management applications, provided it is properly adjusted to local conditions.

5 | CONCLUSIONS

Climatic variations, particularly temperature, exert a strong influence on coffee yield, with higher temperatures associated with reduced productivity, especially during sensitive phenological stages such as flowering and fruit filling. Among these stages, fruit filling was identified as the most sensitive to heat, while flowering may face greater risks due to climatic variability.

The Bourbon Vermelho cultivar demonstrates greater resistance to temperature increases during the vegetative period but shows higher sensitivity during the reproductive phase. Therefore, this cultivar may perform better in years with elevated temperatures that coincide primarily with its vegetative period.

The model demonstrated high predictive capacity at the regional scale (R^2 = 0.93; RMSE = 453 kg ha^{-1}), showing consistency with the observed patterns, but limited performance at the local scale, which highlights the need for improvements in data resolution and quality, as well as methodological adjustments for its application at more detailed levels. Yield losses were mainly associated with water deficit, followed by frost events, while thermal effects were less pronounced.

AUTHOR CONTRIBUTIONS

Marcus Vinicius Oliveira Noronha: Conceptualization; data curation; formal analysis; investigation; methodology; resources; validation; visualization; writing—original draft; writing—review and editing. **João Paulo Silva**: Data curation; formal analysis; methodology; writing—original draft; writing—review and editing. **Marcos Augusto Plachi**: Data curation; project administration. **Douglas Martins de Santana**: Conceptualization; formal analysis; writing—original draft; writing—review and editing. **Renan Caldas Umburanas**: Conceptualization; writing—original draft; writing—review and editing. **José Laércio Favarin**: Conceptualization; visualization; writing—original draft; writing—review and editing. **Luciana Alvim Santos Romani**: Resources; supervision; visualization; writing—review and editing. **Silvia Maria Fonseca Silveira Massruhá**: Funding acquisition; project administration; resources; supervision. **Durval Dourado Neto**: Conceptualization; funding acquisition; methodology; project administration; resources; supervision; visualization; writing—original draft; writing—review and editing.

ACKNOWLEDGMENTS

The authors would like to thank FAPESP for the financial support provided through the Semear Digital project (Processes 2022/09319-9 and 2023/11113-2).

CONFLICT OF INTEREST STATEMENT

The authors declare no conflicts of interest.

DATA AVAILABILITY STATEMENT

The data that support the findings of this study are available from the corresponding author upon reasonable request.

ORCID

Marcus Vinicius Oliveira Noronha https://orcid.org/0009-0004-7935-6380
João Paulo Silva https://orcid.org/0000-0002-0695-9111
Douglas Martins de Santana https://orcid.org/0000-0002-5158-745X
Renan Caldas Umburanas https://orcid.org/0000-0002-4112-3598
José Laércio Favarin https://orcid.org/0000-0003-0556-9397
Luciana Alvim Santos Romani https://orcid.org/0000-0002-7386-3515
Silvia Maria Fonseca Silveira Massruhá https://orcid.org/0000-0002-8055-0680
Durval Dourado Neto https://orcid.org/0000-0002-8452-8288

REFERENCES

Alvares, C. A., Stape, J. L., Sentelhas, P. C., de Moraes Gonçalves, J. L., & Sparovek, G. (2013). Köppen's climate classification map for Brazil. *Meteorologische Zeitschrift*, *22*(6), 711–728. https://doi.org/10.1127/0941-2948/2013/0507

Aparecido, L. E. d. O., Lorençone, J. A., Lorençone, P. A., Torsoni, G. B., Lima, R. F., & dade Silva CabralMoraes, J. R. (2022). Predicting coffee yield based on agroclimatic data and machine learning.

14350645, 2026, 3, Downloaded from https://acsess.onlinelibrary.wiley.com/doi/10.1002/agj2.70458 by EMBRAPA - Empresa Brasileira de Pesquisa Agropecuaria, Wiley Online Library on [22/06/2026]. See the Terms and Conditions (https://onlinelibrary.wiley.com/terms-and-conditions) on Wiley Online Library for rules of use; OA articles are governed by the applicable Creative Commons License

Theoretical and Applied Climatology, *148*, 899–914. https://doi.org/10.1007/s00704-022-03983-z

Batista, L. A., Guimarães, R. J., Pereira, F. J., Carvalho, G. R., & Castro, E. M. (2010). Leaf anatomy and water potential in the coffee cultivars tolerance to water stress. *Revista Ciência Agronômica*, *41*(3), 475–481. https://doi.org/10.1590/S1806-66902010000300022

Bhat, S. A., Qadri, S. A. A., Dubbey, V., Sofi, I. B., & Huang, N. F. (2024). Impact of crop management practices on maize yield: Insights from farming in tropical regions and predictive modeling using machine learning. *Journal of Agriculture and Food Research*, *18*, 101392. https://doi.org/10.1016/j.jafr.2024.101392

Bussoni, C. V. A., Moreira, D. S., & Machado, J. P. (2022). Evaluation of WRF model for application of frost forecast index in the South Brazil. *Revista Brasileira de Meteorologia*, *37*(3), 279–287. https://doi.org/10.1590/0102-77863730084

Camargo, A. P., & Camargo, M. B. P. (2001). Definition and outline for the phenological phases of arabic coffee under Brazilian tropical conditions. *Bragantia*, *60*(1), 65–68. https://doi.org/10.1590/S0006-87052001000100008

Carvalho, H. P., Melo, B., Rabelo, P. G., Silva, C. R., & Camargo, R. (2011). Bioclimatic indices for the coffee crop. *Revista Brasileira de Engenharia Agrícola e Ambiental*, *15*(6), 601–606. https://doi.org/10.1590/S1415-43662011000600010

Carvalho, L. G., Sediyama, G. C., Cecon, P. R., & Alves, H. M. R. (2003). Avaliação de um modelo agrometeorológico para a previsão de produtividade de café em três localidades da região sul do estado de Minas Gerais. *Revista Brasileira de Agrometeorologia*, *11*(2), 323–331.

Companhia Nacional de Abastecimento. (2025). *Safras: Café*. https://www.conab.gov.br/informacoes-agropecuarias/safras/cafe

Dias, C. G., Martins, F. M., & Martins, M. A. (2024). Climate risks and vulnerabilities of the Arabica coffee in Brazil under current and future climates considering new CMIP6 models. *Science of the Total Environment*, *907*, 167753. https://doi.org/10.1016/j.scitotenv.2023.167753

Du, Y., Zhao, Q., Chen, L., Yao, X., Zhang, H., Wu, J., & Xie, F. (2020). Effect of drought stress during soybean R2–R6 growth stages on sucrose metabolism in leaf and seed. *International Journal of Molecular Sciences*, *21*(2), 618. https://doi.org/10.3390/ijms21020618

Fattah, M. D. A., Hasan, M. M., Dola, I. A., Morshed, S. R., Chakraborty, T., Kafy, A., Alsulamy, S., Khedher, K. M., & Shohan, A. A. A. (2024). Implications of rainfall variability on groundwater recharge and sustainable management in South Asian capitals: An in-depth analysis using Mann Kendall tests, continuous wavelet coherence, and innovative trend analysis. *Groundwater for Sustainable Development*, *24*, 101060. https://doi.org/10.1016/j.gsd.2023.101060

Freitas, C. H., Coelho, R. D., de Oliveira Costa, J., & Sentelhas, P. C. (2024). A bitter cup of coffee? Assessing the impact of climate change on Arabica coffee production in Brazil. *Science of the Total Environment*, *957*, 177546. https://doi.org/10.1016/j.scitotenv.2024.177546

Freitas, C. H., Coelho, R. D., de Oliveira Costa, J., & Sentelhas, P. C. (2025). Equationing Arabica coffee: Adaptation, calibration, and application of an agrometeorological model for yield estimation. *Agricultural Systems*, *223*, 104181. https://doi.org/10.1016/j.agsy.2024.104181

Han, S., Li, D., Li, K., Wu, H., Gao, Y., Zhang, Y., & Yuan, R. (2024). Analysis and study of transmission line icing based on grey correlation Pearson combinatorial optimization support vector machine. *Measurement*, *236*, 115086. https://doi.org/10.1016/j.measurement.2024.115086

Humphries, U. W., Waqas, M., Hlaing, P. T., Wangwongchai, A., & Dechpichai, P. (2024). Determination of crop water requirements and potential evapotranspiration for sustainable coffee farming in response to future climate change scenarios. *Smart Agricultural Technology*, *8*, 100435. https://doi.org/10.1016/j.atech.2024.100435

Instituto Brasileiro de Geografia e Estatística. (2025). *SIDRA – Sistema IBGE de Recuperação Automática*. https://sidra.ibge.gov.br

International Coffee Organization. (2026). *Public market information*. https://ico.org/resources/public-market-information/

Instituto Nacional de Meteorologia. (2025). *Estações Meteorológicas*. https://portal.inmet.gov.br/paginas/catalogo

Kendall, M. G. (1975). *Rank correlation methods* (4th ed.). Griffin.

Liu, R., Yang, C., Zhang, G., Zhang, L., Yang, F., & Guo, W. (2015). Root recovery development and activity of cotton plants after waterlogging. *Agronomy Journal*, *107*(6), 2038–2046. https://doi.org/10.2134/agronj14.0567

Mann, H. B. (1945). Nonparametric tests against trend. *Econometrica*, *13*(3), 245. https://doi.org/10.2307/1907187

Mehrotra, R., Verma, R. K., & Pal, A. (2022). Iron deficiency chlorosis in aromatic grasses: A review. *Environmental Challenges*, *9*, 100646. https://doi.org/10.1016/j.envc.2022.100646

Monteiro, J. E. B. A.(2009). *Agrometeorologia dos cultivos: O fator meteorológico na produção agrícola*. INMET.

Pereira, A. R., Camargo, Â. P., & Camargo, M. B. P. (2008). *Agrometeorologia de cafezais no Brasil*. Instituto Agronômico.

Pezzopane, J. R. M., Pedro Júnior, M. J., Camargo, M. B. P., & Fazuoli, L. C. (2008). Heat requeriments of Mundo Novo coffee for the flowering-harvest phenological stage. *Ciência e Agrotecnologia*, *32*(6), 1781–1786. https://doi.org/10.1590/S1413-70542008000600016

Picini, A. G., Camargo, M. B. P., Ortolani, A. A., Fazuoli, L. C., & Gallo, P. B. (1999). Test and analysis of agrometeorological models for predicting coffee yield. *Bragantia*, *58*(1), 157–170. https://doi.org/10.1590/S0006-87051999000100015

Roman, M., Li, M., Yuan, J., Rehman, M., & Liu, L. (2024). Dynamics of industrial hemp vegetative growth and metabolite accumulation in response to light intensity. *South African Journal of Botany*, *169*, 82–94. https://doi.org/10.1016/j.sajb.2024.04.002

Salazar-Navarro, A., Ruiz-Valdiviezo, V., Joya-Dávila, J., & Gonzalez-Mendoza, D. (2024). Coffee leaf rust (*Hemileia vastatrix*) disease in coffee plants and perspectives by the disease control. *Phyton-International Journal of Experimental Botany*, *93*, 923–949. https://doi.org/10.32604/phyton.2024.049612

Santos, M. A., & Camargo, M. B. P. (2006). Parametrização de modelo agrometeorológico de estimativa de produtividade do cafeeiro nas condições do Estado de São Paulo. *Bragantia*, *65*(1), 173–183. https://doi.org/10.1590/S0006-87052006000100022

Shuman, L. M. (2005). Micronutrients. In D. Hillel (Ed.), *Encyclopedia of soils in the environment* (pp. 479–486). Elsevier. https://doi.org/10.1016/B0-12-348530-4/00231-9

Streck, N. A., Silva, S. D. D., & Langner, J. A. (2012). Assessing the response of maize phenology under elevated temperature scenarios. *Revista Brasileira de Meteorologia*, *27*(1), 1–12. https://doi.org/10.1590/S0102-77862012000100001

Tavares, P. D. S., Giarolla, A., Chou, S. C., Silva, A. J. D. P., & Lyra, A. D. A. (2018). Climate change impact on the potential yield of Arabica

14350645, 2026, 3, Downloaded from https://acsess.onlinelibrary.wiley.com/doi/10.1002/agj2.70458 by EMBRAPA - Empresa Brasileira de Pesquisa Agropecuaria, Wiley Online Library on [22/06/2026]. See the Terms and Conditions (https://onlinelibrary.wiley.com/terms-and-conditions) on Wiley Online Library for rules of use; OA articles are governed by the applicable Creative Commons License

coffee in southeast Brazil. *Regional Environmental Change*, *18*, 873–883. https://doi.org/10.1007/s10113-017-1236-z

Thornthwaite, C. W. (1948). An approach toward a rational classification of climate. *Geographical Review*, *38*(1), 55. https://doi.org/10.2307/210739

Thornthwaite, C. W., & Mather, J. R. (1955). *The water balance*. Laboratory of Climatology.

Torres, R. R., Benassi, R. B., Martins, F. B., & Lapola, D. M. (2022). Projected impacts of 1.5 and 2°C global warming on temperature and precipitation patterns in South America. *International Journal of Climatology*, *42*(3), 1597–1611. https://doi.org/10.1002/joc.7322

Valeriano, T. T. B., de Souza Rolim, G., de Oliveira Aparecido, L. E., & de Moraes, J. R. D. S. C. (2018). Estimation of coffee yield from gridded weather data. *Agronomy Journal*, *110*, 2462–2477. https://doi.org/10.2134/agronj2017.11.0649

Verhage, F. Y. F., Anten, N. P. R., & Sentelhas, P. C. (2017). Carbon dioxide fertilization offsets negative impacts of climate change on Arabica coffee yield in Brazil. *Climatic Change*, *144*, 671–685. https://doi.org/10.1007/s10584-017-2068-z

Wu, F., Guo, S., Huang, W., Zhang, Z., Han, Y., Wang, Z., Wang, G., Feng, L., Li, X., Lei, Y., Zhi, X., Yang, B., Zhang, S., Xiong, S., Jiao, Y., Xin, M., & Li, Y. (2024). Extreme rainfall and soil water consumption differences increase yield shedding at lower fruiting branches, reducing cotton water yield under different sowing dates. *Agricultural Water Management*, *305*, 109115. https://doi.org/10.1016/j.agwat.2024.109115

Wu, J., Chen, X., Yu, Z., Yao, H., Li, W., & Zhang, D. (2019). Assessing the impact of human regulations on hydrological drought development and recovery based on a 'simulated-observed' comparison of the SWAT model. *Journal of Hydrology*, *577*, 123990. https://doi.org/10.1016/j.jhydrol.2019.123990

Xie, X., & Li, A. (2020). An adjusted two-leaf light use efficiency model for improving GPP simulations over mountainous areas. *Journal of Geophysical Research: Atmospheres*, *125*, e2019JD031702. https://doi.org/10.1029/2019JD031702

Zacharias, A. O., Camargo, M. B. P., & Fazuoli, L. C. (2008). Agrometeorological model for estimating the beginning of the flowering period for coffee crop (*Coffea arabica* L.). *Bragantia*, *67*(1), 249–256. https://doi.org/10.1590/S0006-87052008000100030

SUPPORTING INFORMATION

Additional supporting information can be found online in the Supporting Information section at the end of this article.

How to cite this article: Noronha, M. V. O., Silva, J. P., Plachi, M. A., Santana, D. M., Umburanas, R. C., Favarin, J. L., Romani, L. A. S., Massruhá, S. M. F. S., & Dourado Neto, D. (2026). Thermal sensitivity and yield of Arabica coffee under climatic variability. *Agronomy Journal*, *118*, e70458. https://doi.org/10.1002/agj2.70458

14350645, 2026, 3, Downloaded from https://acsess.onlinelibrary.wiley.com/doi/10.1002/agj2.70458 by EMBRAPA - Empresa Brasileira de Pesquisa Agropecuaria, Wiley Online Library on [22/06/2026]. See the Terms and Conditions (https://onlinelibrary.wiley.com/terms-and-conditions) on Wiley Online Library for rules of use; OA articles are governed by the applicable Creative Commons License